Electronic Supporting Information

Phosphorescent 2-phenylbenzothiazole Pt^{IV} bis-cyclometalated complexes with phenanthroline-based ligands

Andrea Corral-Zorzano, David Gómez de Segura, Elena Lalinde* and Mª Teresa Moreno*

Departamento de Química-Centro de Síntesis Química de La Rioja, (CISQ), Universidad de La Rioja, 26006, Logroño, Spain. E-mail: elena.lalinde@unirioja.es; teresa.moreno@unirioja.es

Contents: Page

1. Experimental Section

General Comments. All reactions were carried out under an atmosphere of dry nitrogen, using standard Schlenk techniques. Solvents were obtained from a solvent purification system (M-BRAUN MS SPS-800). Elemental analyses were carried out with a EA FLASH 2000 (Thermo Fisher Scientific) microanalyzer. Mass spectra were recorded on a Microflex MALDI-TOF Bruker (MALDI) spectrometer operating in the linear and reflector modes using dithranol as the matrix. IR spectra were obtained on a Fourier Transform Perkin Elmer Spectrum UATR Two spectrophotometer, with the diamond crystal ATR attachment, which covers the region between 4000 and 450 cm^{-1}; data processing was carried out with Omnic. NMR spectra were recorded on a Bruker AVANCE ARX 400 spectrometer at 298 K. Chemical shifts are reported in parts per million (ppm) relative to external standards ($SiMe_4$ for ^1H and $^{13}C\{^1H\}$ and $CFCl_3$ for $^{19}F\{^1H\}$) and all coupling constants are given in hertz (Hz). The UV-Vis absorption spectra were measured with a Hewlett Packard 8453 spectrophotometer. Excitation and emission spectra were obtained with a Shimazdu RF-60000 and Edimburg FLS 1000 spectrofluorimeters. Lifetime measurements were performed with Edimburg FLS 1000 spectrofluorimeter with μF2 pulse lamp (Power: 100 W, Fuse: 3.15 Amp A/S); the estimated uncertainty is ±10% or better. Quantum Yields were measured with Hamamatsu Absolute PL Quantum Yield Spectrometer; the estimated uncertainty is ±5% or better. Cyclic voltammograms were registered on a potenciostat Voltalab PST 050 with the CV cell consisting of a platinum disk as working electrode, a Pt wire counter electrode and an Ag/AgCl reference electrode. The measurements were carried out at 298 K under N_2 atmosphere, using degassed 5 x 10^{-4} M solutions of the complexes in dry CH_2Cl_2 and 0.1 M $(NBu_4)PF_6$ as the supporting electrolyte. The ferrocene/ferricinium couple served as the internal reference (+0.45 V *vs* Ag/AgCl). $PhICl_2$ was prepared according to the published procedure.[1]

Complex [Pt(pbt)(Hpbt-*κN*)Cl] (**1**) was synthesized following the published procedure[2] and was fully characterized. Elem. Anal. Calcd for $C_{26}H_{17}N_2ClPtS_2$ (652.09): C, 47.89; H, 2.63; N, 4.30; S, 9.83. Found: C, 47.58; H, 2.76; N, 4.78; S, 10.31. MALDI (+): *m/z* (%): 616.019 $[M-Cl]^+$ (100), 651.962 $[M]^+$ (26). IR (cm^{-1}): ν(Pt-Cl) 332 (w), ν(Pt-N) 436 (w). ^1H NMR (400 MHz, $CDCl_3$): δ 9.94 (d, $^3J_{H-H}$ = 8.5, H^7), 9.12 (d, $^3J_{H-H}$ = 8.5, $H^{7'}$), 8.70 (d, 2H, $^3J_{H-H}$ = 7.6, $H^{8'}$), 7.93 (d, $^3J_{H-H}$ = 8.5, H^4), 7.79 (m, $H^{10'}$), 7.53 – 7.60 (m, 5H,

$H^{5,6,4'-6'}$), 7.41 – 7.51 (m, 3H, $H^{9',8}$), 6.99 (t, $^3J_{H-H}$ = 7.5, H^9), 6.77 (t, $^3J_{H-H}$ = 7.5, H^{10}), 6.07 (d, $^3J_{H-H}$ = 8, $^3J_{Pt-H}$ = 46.5, H^{11}).

Synthesis of *cis*-[Pt(pbt)$_2$Cl$_2$] (2). To a yellow suspension of **1** (0.190 g, 0.292 mmol) in 30 mL of CH_2Cl_2 at 0 ºC, $PhICl_2$ (0.105 g, 0.379 mmol) was added. After 6 h of stirring, the solvent was evaporated to dryness and the residue treated with Et_2O (15 mL) to obtain **2** as a pale-yellow solid (0.185 g, 93 %). Elem. Anal. Calcd for $C_{26}H_{16}Cl_2N_2PtS_2$ (686,53): C, 45.49; H, 2.35; N, 4.08; S, 9.34. Found: C, 45.01; H, 2.47; N, 3.98; S, 8.94. MALDI (+): *m/z* (%) 651.088 $[M-Cl]^+$ (100), 709.098 $[M+Na]^+$ (18). IR (cm^{-1}): ν(Pt-Cl) 332 (m), ν(Pt-N) 461(m). ^1H NMR (400 MHz, DMSO-d^6): δ 9.84 (d, $^3J_{H-H}$ = 8.5, H^7), 8.45 (d, $^3J_{H-H}$ = 8.3, H^4), 7.99 (d, $^3J_{H-H}$ = 7.6, H^8), 7.79 – 7.71 (m, 2H, $H^{5,6}$), 7.24 (t, $^3J_{H-H}$ = 7.6, H^9), 7.05 (t, $^3J_{H-H}$ = 7.6, H^{10}), 6.16 (d, $^3J_{H-H}$ = 8.1, $^3J_{Pt-H}$ = 31.4, H^{11}).

Synthesis of *cis*-[Pt(pbt)$_2$(OCOCF$_3$)$_2$] (3). A mixture of **2** (0.264 g, 0.384 mmol) and silver trifluoroacetate (0.180 g, 0.814 mmol) was refluxed in 40 mL of acetone. After 6 h, the suspension was filtered through celite and the filtrate was evaporated to dryness. The residue was dissolved in 2 mL of $CHCl_3$ and treated with *n*-hexane (10 mL) to obtain **3** as a pale-yellow solid (0.192 g, 59 %). Elem. Anal. Calcd for $C_{30}H_{16}F_6N_2O_4PtS_2$ (841,66): C, 42.81; H, 1.92; N, 3.33; S, 7.62. Found: C, 42.37; H, 1.87; N, 3.20; S, 7.65. MALDI (+): *m/z* (%) 616.039 $[M-2CF_3CO_2]^+$ (68), 728.040 $[M-CF_3CO_2]^+$ (100), 865.220 $[M+Na]^+$ (20). IR (cm^{-1}): ν(Pt-N) 451 (m), ν(CO) 1699 (s). ^1H NMR (400 MHz, $CDCl_3$): δ 9.36 (d, $^3J_{H-H}$ = 8.5, H^7), 8.00 (d, $^3J_{H-H}$ = 8.2, H^4), 7.70 (t, $^3J_{H-H}$ = 7.7, H^6), 7.63 (m, 2H, $H^{8,5}$), 7.19 (t, $^3J_{H-H}$ = 7.5, H^9), 6.93 (t, $^3J_{H-H}$ = 7.9, H^{10}), 6.09 (d, $^3J_{H-H}$ = 7.9, $^3J_{Pt-H}$ = 32.5, H^{11}). $^{13}C\{^1H\}$ NMR (100.6 MHz, $CDCl_3$): δ 179.6 (s, J_{Pt-C} = 90.6, C^2), 168.8 (c, J_{C-F} = 37, CO), 147.9 (s, J_{Pt-C} = 33.1, C^{7a}), 137.9 (s, J_{Pt-C} = 21.8, C^{13}), 133.1 (s, J_{Pt-C} = 39.5, C^{10}), 130.7 (s, J_{Pt-C} = 805, C^{12}), 130.0 (s, J_{Pt-C} = 35.6, C^{3a}), 129.2 (s, C^6), 128.4 (s, J_{Pt-C} = 26.4, C^{11}), 127.4 (m , $C^{8,9}$), 126.8 (s, J_{Pt-C} = 26.8, C^5), 122.7 (s, C^4), 122.1 (s, C^7), 116.4 (c, J_{C-F} = 292, CF_3). $^{19}F\{^1H\}$ NMR (282.4 MHz, $CDCl_3$): δ -74.9 (s, $^4J_{Pt-F}$ = 4.6 Hz).

Synthesis of [Pt(pbt)$_2$(phen)](CF$_3$CO$_2$)$_2$ (4-CF$_3$CO$_2$). 1,10-phenanthroline (0.022 g, 0.123 mmol) was added to a solution of **3** (0.102 g, 0.121 mmol) in 15 mL of CH_2Cl_2 and the solution was stirred for 3 h. Then, the solvent was removed to 2 mL and treated with *n*-hexane (10 mL) to obtain **4-CF$_3$CO$_2$** as a pale-orange solid (0.101 g, 77 %). Elem. Anal. Calcd for $C_{42}H_{24}F_6N_4O_4PtS_2$ (1021,87): C, 49.37; H, 2.37; N, 5.48; S, 6.27. Found: C, 49.89; H, 2.23; N, 4.98; S, 5.73. MALDI (+): *m/z* (%) 903.029 $[M-CF_3CO_2]^+$ (32),

795.108 [M-2CF_3CO_2]$^+$ (19), 728.014 [M-phen-CF_3CO_2]$^+$ (55), 585.059 [M-pbt-2CF_3CO_2]$^+$ (100). IR (cm^{-1}): ν(Pt-N) 453 (m), ν(CO) 1699 (s). ^{1}H NMR (400 MHz, $CDCl_3$): δ 9.36 (d, $^3J_{H-H}$ = 8.4, H^7), 9.17 (d, $^3J_{H-H}$ = 4.1, H$^{1'}$), 8.33 (d, $^3J_{H-H}$ = 8.3, H$^{3'}$), 7.99 (d, $^3J_{H-H}$ = 7.9, H^4), 7.87 (s, H$^{5'}$), 7.71 (m, 2H, H$^{6,2'}$), 7.62 (m, 2H, H^8, H^5), 7.18 (t, $^3J_{H-H}$ = 7.4, H^9), 6.93 (t, $^3J_{H-H}$ = 7.7, H^{10}), 6.1 (d, $^3J_{H-H}$ = 7.9, $^3J_{Pt-H}$ = 32.6, H^{11}). ^{13}C{^{1}H} NMR (100.6 MHz, $CDCl_3$): δ 179.5 (s, $^3J_{Pt-C}$ = 91.3, C^2), 168.8 (c, J_{C-F} = 37, CO), 150.6 (s, C$^{1'}$), 147.8 (s, $^3J_{Pt-C}$ = 32.9, C^{7a}), 145.5 (s, C$^{12'}$), 137.8 (s, $^3J_{Pt-C}$ = 21.7, C^{13}), 136.6 (s, C$^{3'}$), 132.9 (s, $^3J_{Pt-C}$ = 39.5, C^{10}), 130.6 (s, C^{12}), 129.9 (s, $^3J_{Pt-C}$ = 36.9, C^{3a}), 129.1 (s, C^6), 128.9 (s, C$^{4'}$), 128.3 (s, $^3J_{Pt-C}$ = 26.3, C^{11}), 127.3 (s, C^{8,9}), 126.8 (s, C^5), 126.7 (s, C$^{5'}$), 123.6 (s, C^2), 122.6 (s, C^4), 122.0 (s, C^7), 116.4 (c, J_{C-F} = 292, CF_3). ^{19}F{^{1}H} NMR (376.5 MHz, $CDCl_3$): δ -74.9 (s, -CF_3).

Synthesis of [Pt(pbt)$_2$(pyraphen)](CF_3CO_2)$_2$ (5-CF_3CO_2). This complex was obtained as a pale-orange solid (0.104 g, 75 %) following the same procedure as **5-CF_3CO_2** starting from **3** (0.102 g, 0.121 mmol) and pyrazino[*2,3-f*][1,10]-phenanthroline (0.029 g, 0.121 mmol). Elem. Anal. Calcd for $C_{44}H_{24}F_6N_6O_4PtS_2$ (1073,91): C, 49.21; H, 2.25; N, 7.83; S, 5.97. Found: C, 49.09; H, 2.20; N, 7.83; S, 5.48. MALDI (+): *m/z* (%) 847.135 [M-2CF_3CO_2]$^+$ (55), 728.022 [M-pyraphen-CF_3CO_2]$^+$ (69), 637.069 [M-pbt-2CF_3CO_2]$^+$ (100), 571.029 [M-pyraphen-2CF_3CO_2]$^+$ (55). IR (cm^{-1}): ν(Pt-N) 442(m), ν(CO) 1697 (s). ^{1}H NMR (400 MHz, $CDCl_3$): δ 9.50 (d, $^3J_{H-H}$ = 8.3, H$^{3'}$), 9.35 (d, $^3J_{H-H}$ = 8.7, H^7), 9.30 (d, $^3J_{H-H}$ = 4.2, H$^{1'}$), 8.99 (s, H$^{6'}$), 7.98 (d, $^3J_{H-H}$ = 8.1, H^4), 7.81 (dd, $^3J_{H-H}$ = 8.1, 4.2, H$^{2'}$), 7.69 (t, $^3J_{H-H}$ = 7.6, H^6), 7.62 (m, H^8, H^5), 7.18 (t, $^3J_{H-H}$ = 7.4, H^9), 6.92 (t, $^3J_{H-H}$ = 7.8, H^{10}), 6.08 (d, $^3J_{H-H}$ = 8.8, $^3J_{Pt-H}$ = 32.5, H^{11}). ^{13}C{^{1}H} NMR (100.6 MHz, $CDCl_3$): δ 179.6 (s, $^3J_{Pt-C}$ = 90, C^2), 168.8 (c, J_{C-F} = 37, CO), 152.5 (s, C$^{1'}$), 147.8 (s, $^3J_{Pt-C}$ = 30.9, C^{7a}), 147.6 (s, C$^{12'}$), 144.7 (s, C$^{6'}$), 140.7 (s, C$^{5'}$), 137.9 (s, $^3J_{Pt-C}$ = 21.6, C^{13}), 133.4 (s, C$^{3'}$), 133.1 (s, $^3J_{Pt-C}$ = 39.1, C^{10}), 130.7 (s, $^1J_{Pt-C}$ ~780, C^{12}), 130.0 (s, $^3J_{Pt-C}$ = 36.5, C^{3a}), 129.2 (s, C^6), 128.4 (s, $^3J_{Pt-C}$ = 26.3, C^{11}), 127.4 (m, C^{8,9}), 127.2 (s, C$^{4'}$), 126.8 (s, $^3J_{Pt-C}$ = 27.2, C^5), 124.2 (s, C$^{2'}$), 122.7 (s, C^4), 122.1 (s, C^7), 116.4 (c, J_{C-F} = 292, CF_3). ^{19}F{^{1}H} NMR (376.5 MHz, $CDCl_3$): δ -74.9 (s, -CF_3).

Synthesis of [Pt(pbt)$_2$(NH_2-phen)](CF_3CO_2)$_2$ (6-CF_3CO_2). 5-amine-1,10-phenanthroline (0.018 g, 0.093 mmol) dissolved in ^{i}PrOH (10 mL) was added to a solution of **3** (0.076 g, 0.091 mmol) in 20 mL of CH_2Cl_2 and the mixture was refluxed for 48 h. Then, the suspension was evaporated to dryness and the residue was extracted with acetone (20 mL) and filtered through celite. The filtrate was evaporated to dryness and

the oil was treated with Et_2O (4 x 5 mL) to obtain **6-CF_3CO_2** as a dark-orange solid (0.068 g, 73 %). Elem. Anal. Calcd for $C_{42}H_{25}F_6N_5O_4PtS_2$ (1036,89): C, 48.65; H, 2.43; N, 6.75; S, 6.18. Found: C, 48.25; H, 2.72; N, 6.94; S, 5.90. MALDI (+): *m/z* (%) 810.109 [M-$2CF_3CO_2$]$^+$ (100), 600.040 [M-pbt-$2CF_3CO_2$]$^+$ (49). IR (cm^{-1}): ν(Pt-N) 451 (m), ν(CO) 1687 (s). ^{1}H NMR (400 MHz, CD_3COCD_3): δ 9.98 (d, $^3J_{H-H}$ = 8.4, H$^{8''}$), 8.78 (d, $^3J_{H-H}$ = 5.3, $^3J_{Pt-H}$ = 15.1 H$^{10''}$), 8.64 (d, $^3J_{H-H}$ = 8.4, H$^{3''}$), 8.40 – 8.34 (m, 4H, H$^{8,8',4,4'}$), 8.29 (d, $^3J_{H-H}$ = 5.3, $^3J_{Pt-H}$ = 15.4, H$^{1''}$), 8.19 (dd, $^3J_{H-H}$ = 8.4, $^3J_{H-H}$ = 5.3, H$^{9''}$), 7.96 (dd, $^3J_{H-H}$ = 8.4, $^3J_{H-H}$ = 5.3, H$^{2''}$), 7.69 (s br, NH_2), 7.62 (2 t, $^3J_{H-H}$ = 7.4, H$^{9,9'}$), 7.46 (2 t, $^3J_{H-H}$ = 7.4, H$^{5,5'}$), 7.39 (s, H$^{6''}$), 7.34 (2 t, $^3J_{H-H}$ = 7.4, H$^{10,10'}$), 7.17 (2 t, $^3J_{H-H}$ = 7.4, H$^{6,6'}$), 6.68, 6.64 (2d, $^3J_{H-H}$ = 8, $^3J_{Pt-H}$ = 28.8, H$^{11,11'}$), 6.06 (d, $^3J_{H-H}$ = 8.6, H^7), 5.97 (d, $^3J_{H-H}$ = 8.6, H$^{7'}$). ^{13}C{^{1}H} NMR (100.6 MHz, CD_3COCD_3): δ 182.6, 182.3 (2 s, $^2J_{Pt-C}$ = 75, C$^{2,2'}$), 151.3 (s, $^3J_{Pt-C}$= 18.2, C$^{10''}$), 148.6 (s, C$^{12''}$), 147.4 (s, C$^{5''}$), 146.0 (2 s, $^3J_{Pt-C}$= 34.8, C$^{7a,7a'}$), 145.3 (s, $^3J_{Pt-C}$= 17.4, C$^{1''}$), 141.0 (s, C$^{8''}$), 140.0 (s, C$^{3''}$), 139.4 (s, C$^{11''}$), 138.1, 137.9 (2 s, $^3J_{Pt-C}$= 17.4, C$^{3a,3a'}$), 137.3, 137.0 (2 s, C$^{12,12'}$), 136.1 (2 s, $^3J_{Pt-C}$= 34.8, C$^{10,10'}$), 136.0 (s, C$^{4''}$), 132.5, 132.3 (C$^{13,13'}$), 130.8, 130.7, 130.6, 130.5 (4 s, C$^{11,11',6,6'}$), 103.2 – 130.1 (4 s, C$^{9,9',8,8'}$), 128.8 (s, $^3J_{Pt-C}$= 17.1, C$^{2''}$), 128.5 (2 s, C$^{5,5'}$), 128 (s, $^3J_{Pt-C}$= 17.1, C$^{9''}$), 126.4 – 126.3 (2 s, C$^{7'',4,4'}$), 117.3 (s, C$^{7,7'}$), 103.3 (s, C$^{6''}$). ^{19}F{^{1}H} NMR (376.5 MHz, CD_3COCD_3): δ = -74.9 (s, -CF_3).

Synthesis of [Pt(pbt)$_2$(phen)](PF_6)$_2$ (4-PF_6). A suspension of [Pt(pbt)$_2$Cl$_2$] (**2**) (0.1412 g, 0.205 mmol), 1,10-phenanthroline (0.0744 g, 0.411 mmol), $TlPF_6$ (0.8740 g, 0.823 mmol) and an excess of $KClO_4$ (0.8521 g, 6.15 mmol) were refluxed in 25 mL of 1,2-dichloroethane for 14 h. Then, the solvent was removed under reduced pressure, the residue treated with CH_2Cl_2 (80 mL) and filtered through celite. The filtrate was evaporated to dryness and treated consecutively with ^{i}PrOH (2 mL) and Et_2O (10 mL) to obtain **4-PF_6** as a pale pink solid (0.171 g, 77 %). Elem. Anal. Calcd for $C_{38}H_{24}F_{12}N_4P_2PtS_2$ (1085.77): C, 42.04; H, 2.23; N, 5.16; S, 5.91. Found: C 41.84; H 2.34; N 4.86; S 5.45. MALDI (+): *m/z* (%) 939.268 [M-PF_6]$^+$ (46), 794.262 [M-2PF_6]$^+$ (100), 614.030 [M-phen-2PF_6]$^+$ (27), 584.096 [M-pbt-2PF_6]$^+$ (34). IR (cm^{-1}): ν(Pt-N) 453 (m), ν(PF_6) 837, 557 (s). ^{1}H NMR (400 MHz, CD_3COCD_3): δ 9.27 (d, $^3J_{H-H}$ = 8.4, H$^{3'}$), 8.95 (d, $^3J_{H-H}$ = 5.3, $^3J_{Pt-H}$ = 15.3, H$^{1'}$), 8.54 (s, H$^{5'}$), 8.39 (m, H^8, H$^{2'}$, H^4), 7.68 (t, $^3J_{H-H}$ = 7.8, H^9), 7.50 (t, $^3J_{H-H}$ = 7.7, H^5), 7.39 (t, $^3J_{H-H}$ = 7.9, H^{10}), 7.15 (t, $^3J_{H-H}$ = 8.3, H^6), 6.73 (d, $^3J_{H-H}$ = 8.0, $^3J_{Pt-H}$ = 28.7, H^{11}), 5.99 (d, $^3J_{H-H}$ = 8.6, H^7). ^{13}C{^{1}H} NMR (100.6 MHz, CD_3COCD_3): δ 182.6 (s, $^2J_{Pt-H}$ = 76.8, C^2), 152.2 (s, $^3J_{Pt-C}$ = 17.5, C$^{1'}$), 146.6 (s, C$^{4'}$),

146.0 (s, $^3J_{Pt-C}$ = 37.6, C^{3a}), 144.3 (s, $C^{3'}$), 138.0 (s, $^3J_{Pt-C}$ = 17.8, C^{13}), 136.6 (s, C^{12}), 136.4 (s, $^3J_{Pt-C}$ = 35, C^{10}), 133.7 (s, $^3J_{Pt-C}$ = 8.8, $C^{12'}$), 132.3 (s, $^3J_{Pt-C}$ = 35.4, C^{7a}), 130.8 (s, C^{11}), 130.7 (s, C^6), 130.5 (s, C^9), 130.4 (s, $C^{5'}$), 130.4 (s, $C^{2'}$), 130.0 (s, $^3J_{Pt-C}$ = 16.8, C^8), 128.7 (s, C^5), 126.2 (s, C^4), 117.3 (s, C^7). $^{19}F\{^1H\}$ NMR (376.5 MHz, CD_3COCD_3): δ -72.5 (d, $^1J_{F-P}$ = 709, PF_6). $^{31}P\{^1H\}$ NMR (161.9 MHz, CD_3COCD_3): δ -144.3 (sept, $^1J_{P-F}$ = 709, PF_6).

Synthesis of [Pt(pbt)$_2$(pyraphen)](PF$_6$)$_2$ (5-PF$_6$). A suspension of [Pt(pbt)$_2$Cl$_2$] (**2**) (0.1426 g, 0.208 mmol), pyrazino[*2,3-f*][1,10]-phenanthroline (0.0581 g, 0.249 mmol), $TlPF_6$ (0.1755 g, 0.498 mmol) and an excess $KClO_4$ (0.8646 g, 6.24 mmol) were refluxed in 10 mL of 1,2-dichloroethane for 24 h. Then, the solvent was removed, the residue treated with CH_3CN (20 mL) and filtered through celite. The filtrate was evaporated to dryness and treated with *n*-hexane (10 mL) to give **5-PF$_6$** as a white solid (0.180 g, 74 %). Elem. Anal. Calcd for $C_{40}H_{24}F_{12}N_6P_2PtS_2$ (1137.81): C, 42.23; H, 2.13; N, 7.39; S, 5.64. Found: C 42.59; H 2.61; N 7.06; S 5.70. MALDI (+): *m/z* (%) 991.137 $[M-PF_6]^+$ (35), 846.135 $[M-2PF_6]^+$ (100), 613.914 [M- pyraphen-$2PF_6$]$^+$ (19). IR (cm^{-1}): ν(Pt-N) 487 (m), ν(PF_6) 839, 555 (s). ^1H NMR (400 MHz, CD_3COCD_3): δ 10.09 (d, $^3J_{H-H}$ = 8.3, $^3J_{Pt-H}$ = 24.3, $H^{3'}$), 9.39 (s, $H^{6'}$), 9.07 (d, $^3J_{H-H}$ = 5.4, $^3J_{Pt-H}$ = 20.1, $H^{1'}$), 8.58 (dd, $^3J_{H-H}$ = 8.6, $^4J_{H-H}$ = 3.2, H^2), 8.41 (d, $^3J_{H-H}$ = 7.8, H^8), 8.33 (d, $^3J_{H-H}$ = 8.4, H^4), 7.70 (t, $^3J_{H-H}$ = 7.8, H^9), 7.48 (t, $^3J_{H-H}$ = 7.9, H^5), 7.40 (t, $^3J_{H-H}$ = 8.4, H^{10}), 7.15 (t, $^3J_{H-H}$ = 8.1, H^6), 6.71 (d, $^3J_{H-H}$ = 8.2, $^3J_{Pt-H}$ = 28.3, H^{11}), 6.16 (d, $^3J_{H-H}$ = 8.6, H^7). $^{13}C\{^1H\}$ NMR (100.6 MHz, CD_3COCD_3): δ 182.7 (s, C^2, pbt), 153.2 (s, $^3J_{Pt-C}$ = 17.3, $C^{1'}$), 148.9 (s, $C^{6'}$), 148.2 (s, $^3J_{Pt-H}$ = 5.1, $C^{12'}$), 146.1 (s, $^3J_{Pt-H}$ = 36.9, C^{7a}), 140.7 (s, $C^{5'}$), 140.4 (s, $^3J_{Pt-H}$ = 30.3, $C^{3'}$), 138.0 (s, 17.9, C^{13}), 136.5 (s, $^4J_{Pt-H}$ = 33.8, C^{10}), 133.1 (s, $C^{4'}$), 132.4 (s, tentatively assigned to C^{12}), 131.4 (s, $^3J_{Pt-H}$ = 15.8, C^{3a}), 130.9 (s, C^{11}), 130.9 (s, $^3J_{Pt-H}$ = 27.2, $C^{2'}$), 130.6, 130.7 (s, $C^{6,9}$), 129.2 (s, $^3J_{Pt-H}$ = 48, C^8), 128.7 (s, C^5), 126.3 (s, C^4), 117.8 (s, C^7). $^{19}F\{^1H\}$ NMR (376.5 MHz, CD_3COCD_3): δ -72.6 (d, $^1J_{F-P}$ = 709, PF_6). $^{31}P\{^1H\}$ NMR (161.9 MHz, CD_3COCD_3): δ -145.3 (sept, $^1J_{P-F}$ =709, PF_6).

Synthesis of [Pt(pbt)$_2$(NH$_2$-phen)](PF$_6$)$_2$ (6-PF$_6$). This complex was obtained as an orange solid (0.1570 g, 73 %) following the same procedure as **4-PF$_6$**, starting of **2** (0.1327 g, 0.195 mmol), 5-amine-1,10-phenanthroline (0.0757 g, 0.388 mmol), $TlPF_6$ (0.2701 g, 0.773 mmol) and an excess $KClO_4$ (0.8105 g, 5.85 mmol). Elem. Anal. Calcd $C_{38}H_{25}F_{12}N_5P_2PtS_2$ (1100.79): C, 41.46; H, 2.29; N, 6.36; S, 5.82. Found: C 41,42; H 2,51; N 6,21; S 5.71. MALDI (+): *m/z* (%) 955.958 $[M-PF_6]^+$ (58), 810.049 $[M-2PF_6]^+$

(100), 615.053 [M- NH_2-phen-2PF_6]$^+$ (6), 600.123 [M-pbt-2PF_6]$^+$ (20). IR (cm^{-1}): ν(Pt-N) 469 (m), ν(PF_6) 841, 557 (s). ^{1}H NMR (400 MHz, CD_3COCD_3): δ 9.38 (d, $^3J_{H-H}$ = 8.6, H$^{8''}$), 8.91 (d, $^3J_{H-H}$ = 5.2, $^3J_{Pt-H}$ = 15.1, H$^{10''}$), 8.77 (d, $^3J_{H-H}$ = 8.5, H$^{3''}$), 8.44 (d, $^3J_{H-H}$ = 5.2, $^3J_{Pt-H}$ = 15.7, H$^{1''}$), 8.35 (m, 5H, H$^{9''}$, H$^{8,8'}$, H$^{4,4'}$), 8.06 (dd, $^3J_{H-H}$ = 8.3, $^4J_{H-H}$ = 3.3, H$^{2''}$), 7.66 (2t, $^3J_{H-H}$ = 7.6, H$^{9,9'}$), 7.53 (t, $^3J_{H-H}$ = 8.0, H$^{5,5'}$), 7.35 (m, H$^{6'',10,10'}$), 7.22, 7.19 (2t, $^3J_{H-H}$ = 8.3, H$^{6,6'}$), 6.76 (s, NH_2), 6.73, 6.68 (2 d, $^3J_{H-H}$ = 8.1, $^3J_{Pt-H}$ = 27.8, H$^{11,11'}$), 6.09 (d, $^3J_{H-H}$ = 8.6, H^7), 6.02 (d, $^3J_{H-H}$ = 8.6, H$^{7'}$). ^{13}C{^{1}H} NMR (100.6 MHz, δ, CD_3COCD_3): δ 182.6 (s, C$^{2,2'}$), 151.75 (s, $^3J_{Pt-C}$=18.2, C$^{1''}$), 147.6 (s, C$^{5''}$), 147.1 (s, C$^{11''}$), 146.5 (s, $^3J_{Pt-C}$ = 17.6 C$^{10''}$), 146.1 (2s, $^3J_{Pt-C}$ = 39.4, C$^{7a,a'}$), 140.5 (s, C$^{8''}$), 140.2 (s, C$^{12''}$), 138.9 (s, C$^{3''}$), 138.0, 137.9 (C$^{13,13'}$), 137.2, 136.8 (tentatively C$^{12,12'}$), 136.4, 136.2 ($^3J_{Pt-C}$ ~ 35 C$^{10,10'}$), 135.8 (s, C$^{7''}$), 132.3, 132.4 (C$^{3a,a'}$), 130.9-130,3 (8s, C$^{6,6',8,8',9,9',11,11'}$), 129.2 (s, $^3J_{Pt-C}$ = 17.6 C$^{2''}$), 128.7 (2 s, C$^{5,5'}$) ,128.4(s, $^3J_{Pt-C}$ = 17.6 C$^{9''}$), 126.2 (3 s, C$^{4'',4,4'}$), 117.4, 117.5 (d, C$^{7,7'}$), 104.5 (s, C$^{6''}$). ^{19}F{^{1}H} NMR (376.5 MHz, CD_3COCD_3): δ -72.5 (d, $^1J_{F-P}$= 709, PF_6). ^{31}P{^{1}H} NMR (161.9 MHz, CD_3COCD_3): δ -144.3 (sept, $^1J_{P-F}$=709, PF_6).

X-ray structure determinations. Yellow (**2**), white (**3**) and yellow (**4-PF$_6$**) crystals were obtained by slow diffusion of ^{i}PrOH into a solution of **2** in $CHCl_3$, of Et_2O into a solution of **3** in CH_2Cl_2 and of *n*-hexane into a solution of (**4-PF$_6$**) in acetone at room temperature. X-ray intensity data were collected using Molybdenum graphite monochromatic (Mo-K$_\alpha$) radiation with a Bruker APEX-II diffractometer at 173 K for **2** and at 298 K for **3** and **4-PF$_6$** using the APEX-II software. Structures were solved by Intrinsic Phasing using SHELXT[3] with the WinGX graphical user interface.[4] Multi-scan absorption corrections were applied to all the data sets and refined by full-matrix least squares on F^2 with SHELXL.[5] Hydrogen atoms were positioned geometrically, with isotropic parameters $U_{iso} = 1.2\ U_{eq}$ (parent atom) for aromatic hydrogens. These complexes crystallized in a centrosymmetric group, so must be aquiral. Thus, both configurations (Λ and Δ) in a 50:50 ratio were found in the unit cell.

Theoretical Calculations. Calculations were carried out with the Gaussian 16 package[6] for **2**, **3**, **4^{2+}-6^{2+}** using Becke´s three-parameter functional combined with Lee-Yang-Parr´s correlation functional (B3LYP).[7] Optimizations on the singlet state (S_0) were performed using as a starting point the molecular geometry obtained through X-ray diffraction analysis for complex **2** and **3** and simulated structures

for **4^{2+}-6^{2+}**. No negative frequency was found in the vibrational frequency analysis of the final equilibrium geometries. The basis set used was the LanL2DZ effective core potential for Pt and 6-31G(d,p) for the ligand atoms.[8] DFT and TD-DFT calculations were carried out using the polarized continuum model approach[9] (PCM) implemented in the Gaussian 16 software, in the presence of CH_2Cl_2. The results were visualized with GaussView 6. Overlap populations between molecular fragments were calculated using the GaussSum 3.0 software.[10]

References

(1) Obeid, N.; Skulski, L. One-Pot Procedures for Preparing (Dichloroiodo)arenes from Arenes and Diiodine, with Chromium(VI) Oxide as the Oxidant. *Molecules* **2001**, *6*, 869-874.

(2) Zhou, Y.; Jia, J.; Cai, L.; Huang, Y. Protein staining agents from low toxic platinum(II) complexes with bidentate ligands. *Dalton Trans.* **2018**, *47*, 693-699.

(3) Sheldrick, G. M. SHELXT – Integrated space-group and crystal structure determination. *Acta Crystallogr., Sect. A: Found. Crystallogr.* **2015**, *71*, 3-8.

(4) Farrugia, L. J. WinGX suite for small-molecule single-crystal crystallography. *Appl. Crystallogr.* **1999**, *32*, 837-838.

(5) Sheldrick, G. Crystal structure refinement with SHELXL. *Acta Crystallogr., Sect. C* **2015**, *71*, 3-8.

(6) M. J. Frisch, G. W. Trucks, H. B. Schlegel, G. E. Scuseria, M. A. Robb, J. R. Cheeseman, G. Scalmani, V. Barone, G. A. Petersson, H. Nakatsuji, X. Li, M. Caricato, A. V. Marenich, J. Bloino, B. G. Janesko, R. Gomperts, B. Mennucci, H. P. Hratchian, J. V. Ortiz, A. F. Izmaylov, J. L. Sonnenberg, D. Williams-Young, F. Ding, F. Lipparini, F. Egidi, J. Goings, B. Peng, A. Petrone, T. Henderson, D. Ranasinghe, V. G. Zakrzewski, J. Gao, N. Rega, G. Zheng, W. Liang, M. Hada, M. Ehara, K. Toyota, R. Fukuda, J. Hasegawa, M. Ishida, T. Nakajima, Y. Honda, O. Kitao, H. Nakai, T. Vreven, K. Throssell, J. A. Montgomery, Jr., J. E. Peralta, F. Ogliaro, M. J. Bearpark, J. J. Heyd, E. N. Brothers, K. N. Kudin, V. N. Staroverov, T. A. Keith, R. Kobayashi, J. Normand, K. Raghavachari, A. P. Rendell, J. C. Burant, S. S. Iyengar, J. Tomasi, M. Cossi, J. M. Millam, M. Klene, C. Adamo, R. Cammi, J. W. Ochterski, R. L. Martin, K. Morokuma, O. Farkas, J. B. Foresman, and D. J. Fox, Gaussian 16, Revision A.03, Inc., Wallingford CT, 2016.

(7) (a) Becke, A. D. Density-functional thermochemistry. III. The role of exact exchange. *J. Chem. Phys.* **1993**, *98*, 5648-5652. (b) Becke, A. D. Density-functional exchange-energy approximation with correct asymptotic behavior. *Phys. Rev. A* **1988**, *38*, 3098-3100.

(8) Wadt, W. R.; Hay, P. J. Ab initio effective core potentials for molecular calculations. Potentials for main group elements Na to Bi. *J. Chem. Phys.* **1985**, *82*, 284-298.

(9) Barone, V.; Cossi, M. Quantum Calculation of Molecular Energies and Energy Gradients in Solution by a Conductor Solvent Model. *J. Phys. Chem. A* **1998**, *102*, 1995-2001.

(10) O'Boyle, N. M.; Tenderholt, A. L.; Langner, K. M. cclib: A library for package-independent computational chemistry algorithms. *J. Comput. Chem.* **2008**, *29*, 839-845.

2. NMR spectra

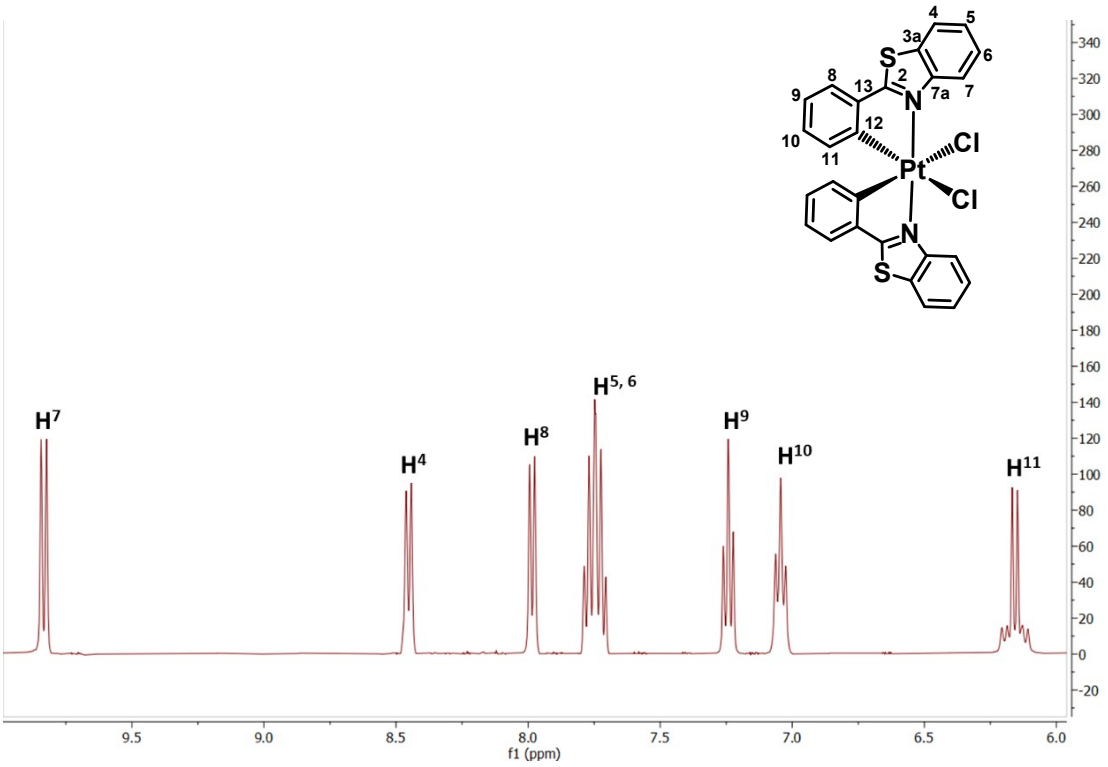

Figure S1. ^{1}H NMR spectra of **2** in DMSO-d^{6} at 298 K

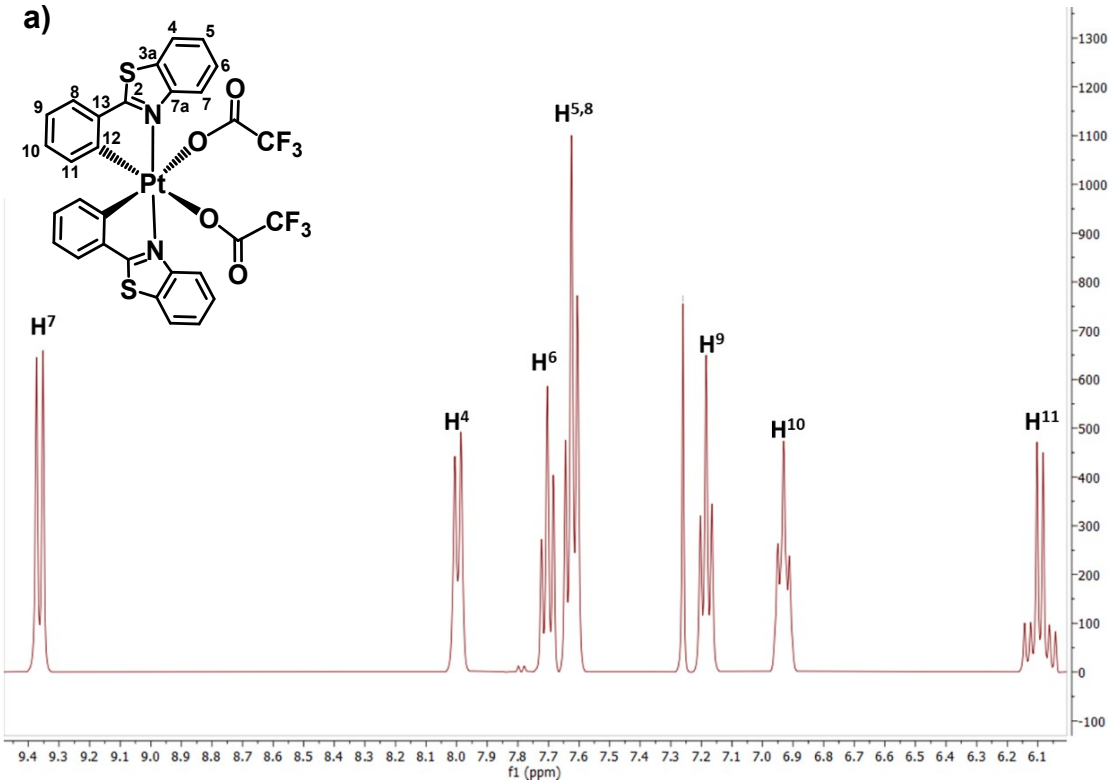

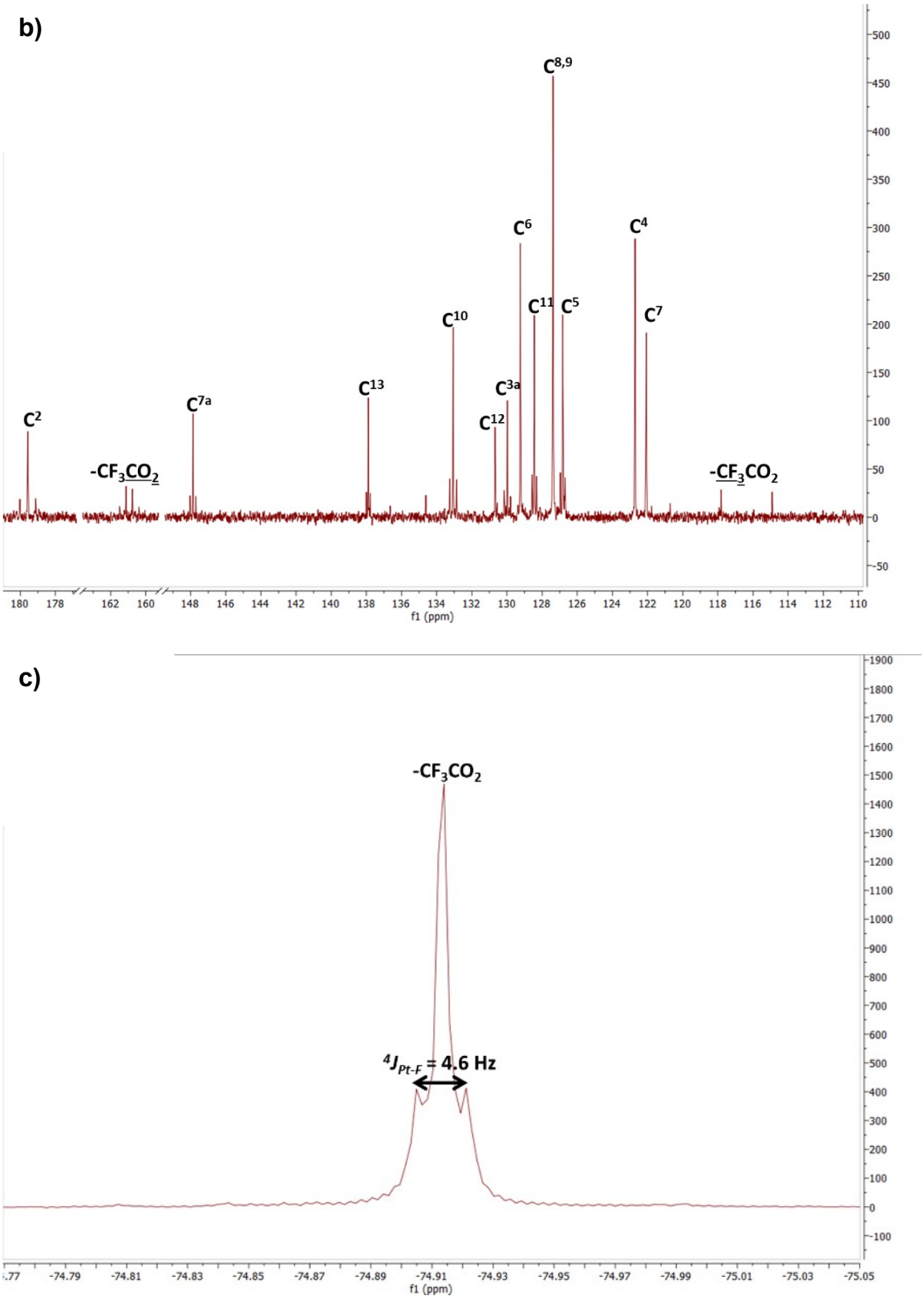

Figure S2. NMR spectra of **3** in $CDCl_3$ at 298 K a) ^{1}H, b) $^{13}C\{^{1}H\}$, c) $^{19}F\{^{1}H\}$

a)

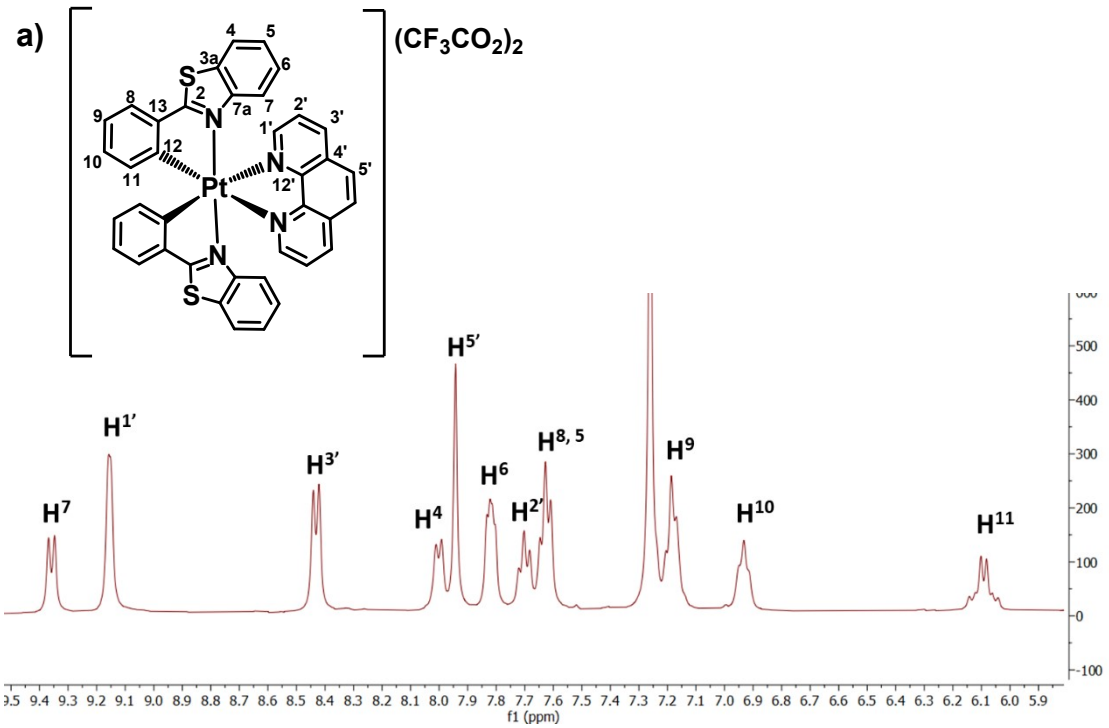
(CF3CO2)2
H7
H1'
H3'
H4
H5'
H6
H2'
H8, 5
H9
H10
H11
f1 (ppm)

b)

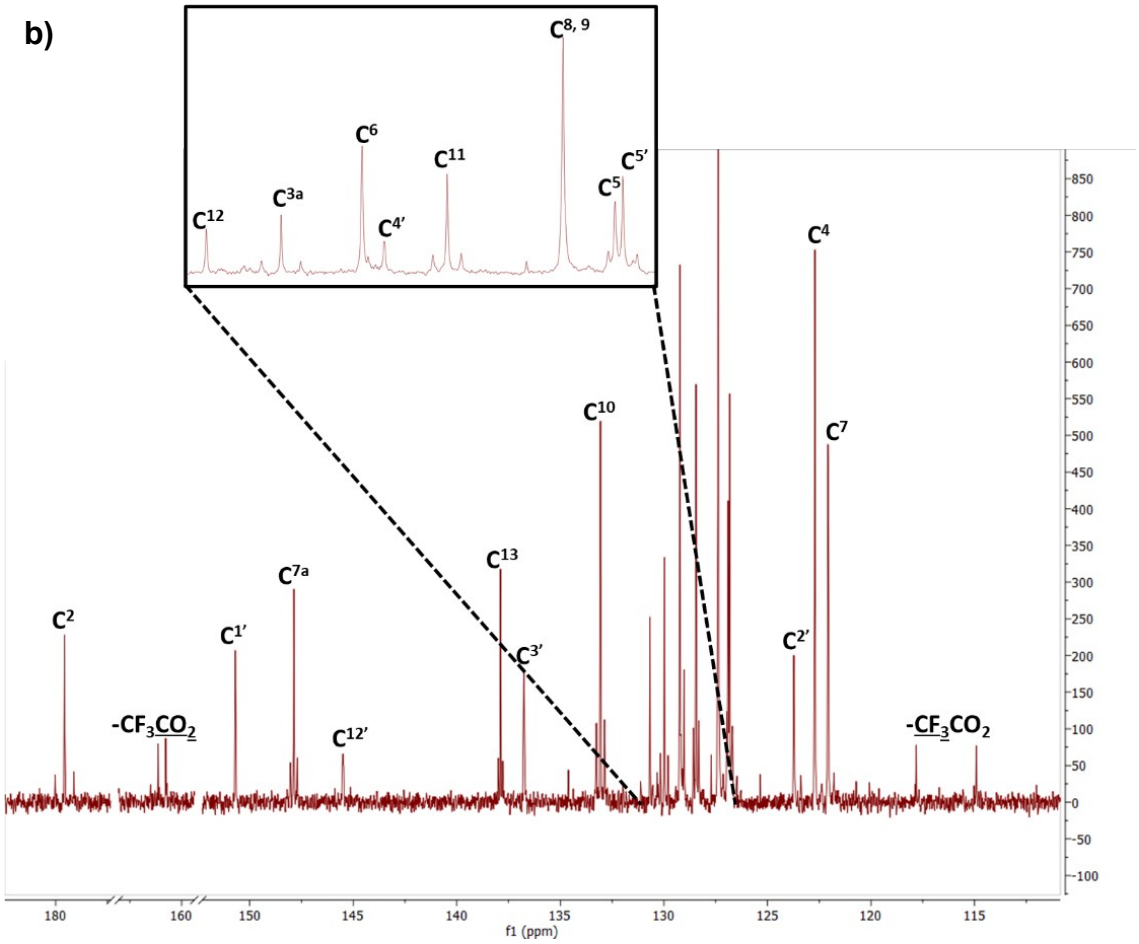
C8, 9
C6
C11
C5'
C5
C3a
C12
C4'
C4
C10
C7
C13
C7a
C2
C1'
C3'
C2'
-CF3CO2
C12'
-CF3CO2
f1 (ppm)

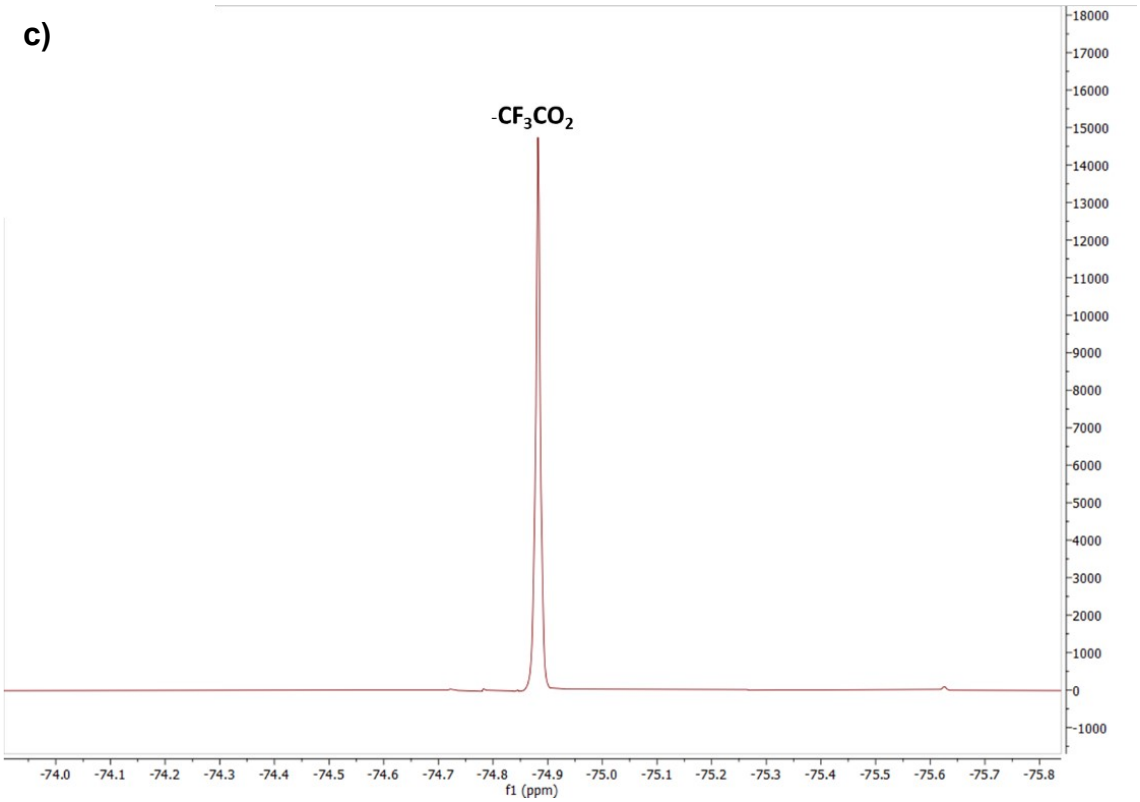

Figure S3. NMR spectra of **4-CF_3CO_2** in $CDCl_3$ at 298 K a) ^{1}H, b) $^{13}C\{^{1}H\}$, c) $^{19}F\{^{1}H\}$

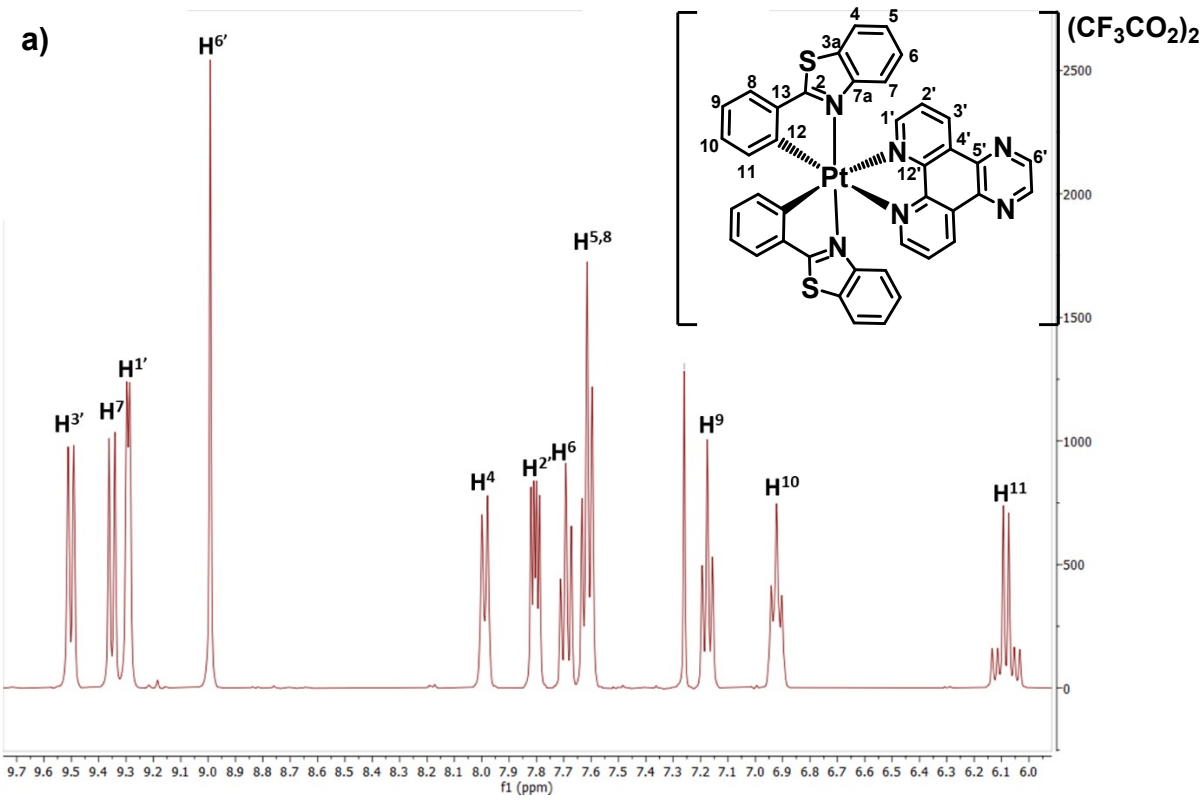
a)
$(CF_3CO_2)_2$
$H^{6'}$
$H^{5,8}$
$H^{1'}$
$H^{3'}$
H^7
H^4
$H^{2'}$
H^6
H^9
H^{10}
H^{11}
f1 (ppm)

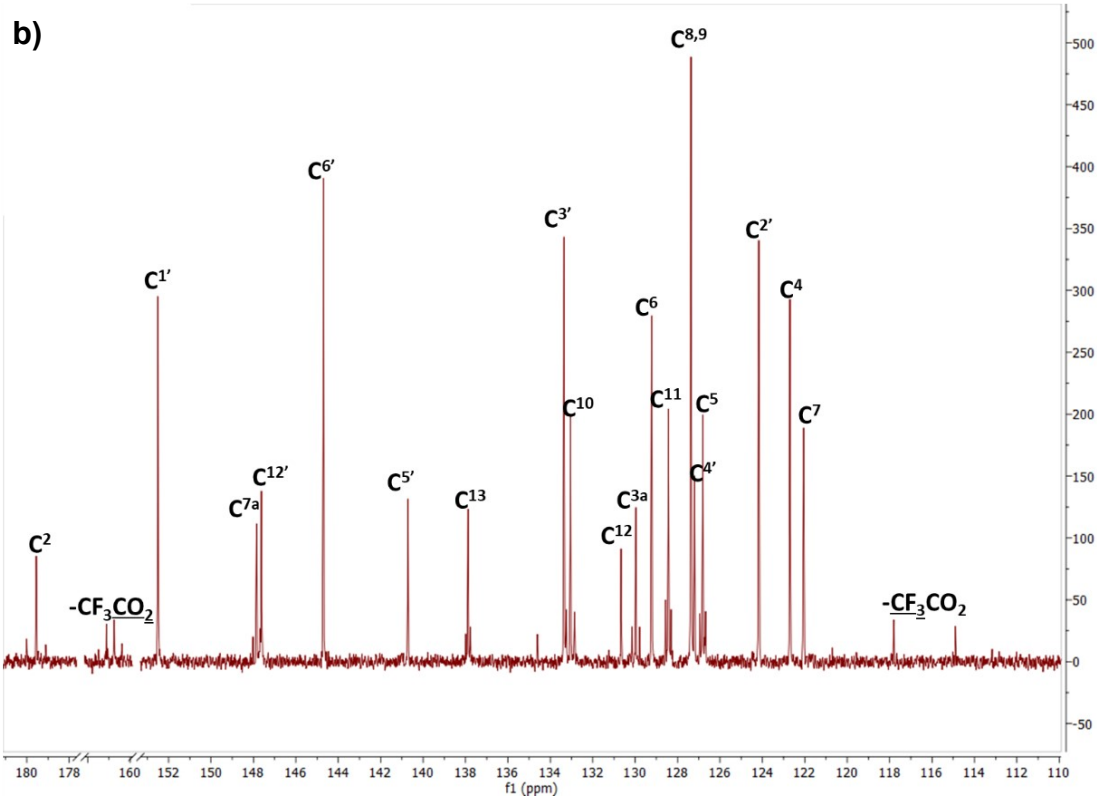
b)
$C^{8,9}$
$C^{6'}$
$C^{3'}$
$C^{2'}$
$C^{1'}$
C^4
C^6
C^{10}
C^{11}
C^5
C^7
$C^{12'}$
$C^{5'}$
C^{13}
C^{3a}
$C^{4'}$
C^{7a}
C^{12}
C^2
$-CF_3CO_2$
$-CF_3CO_2$
f1 (ppm)

c)

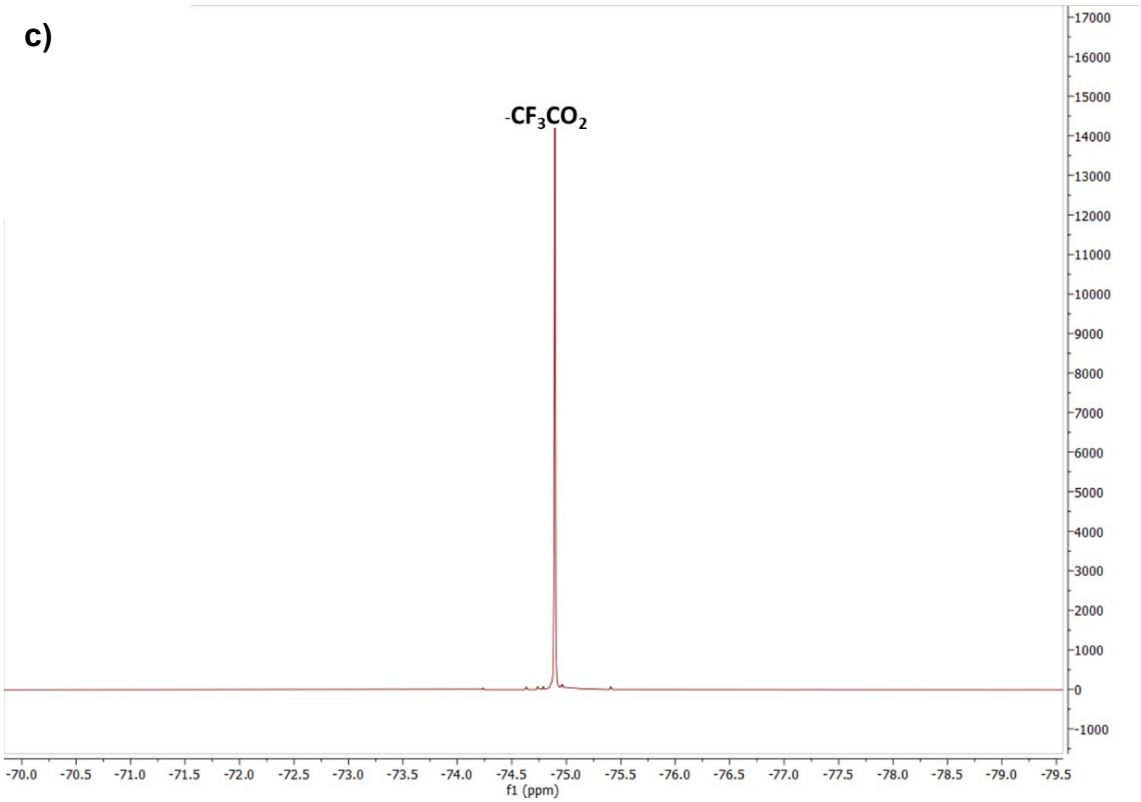

Figure S4. NMR spectra of **5-CF_3CO_2** in $CDCl_3$ at 298 K a) ^{1}H, b) $^{13}C\{^{1}H\}$, c) $^{19}F\{^{1}H\}$

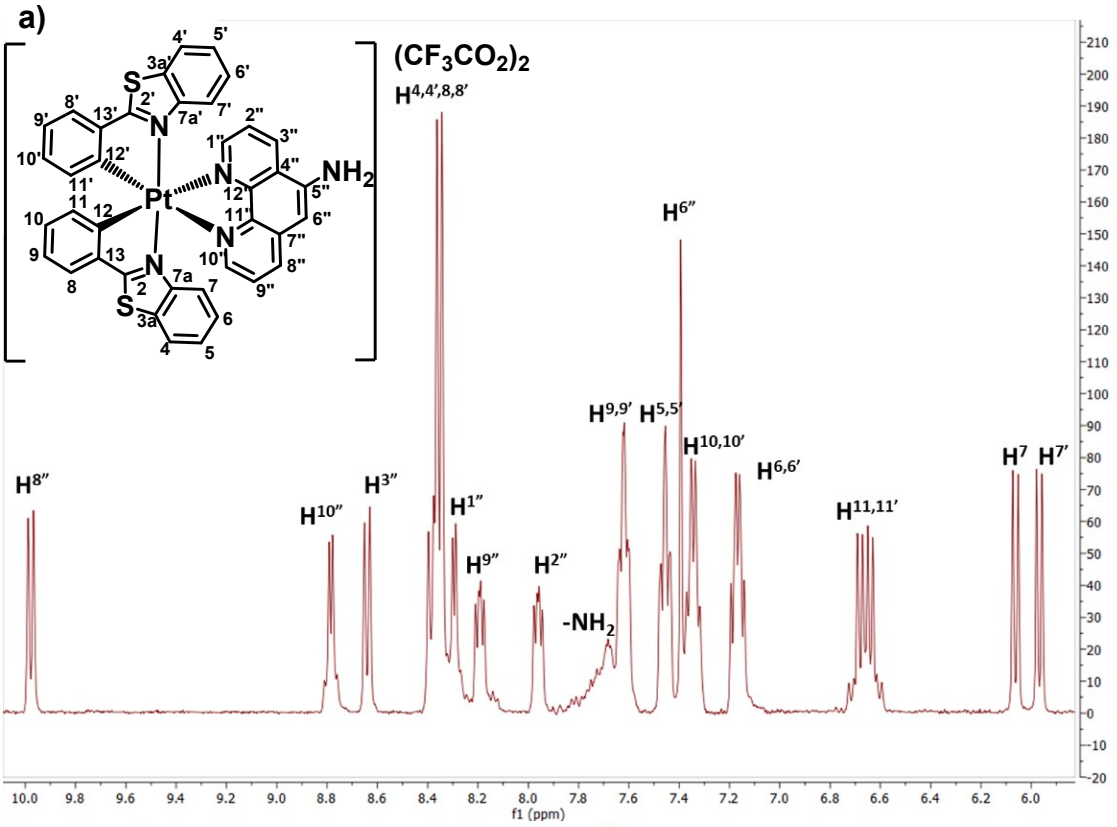
a)
(CF3CO2)2
H4,4',8,8'
H6''
H9,9'
H5,5'
H10,10'
H6,6'
H7
H7'
H8''
H10''
H3''
H1''
H9''
H2''
-NH2
H11,11'
f1 (ppm)

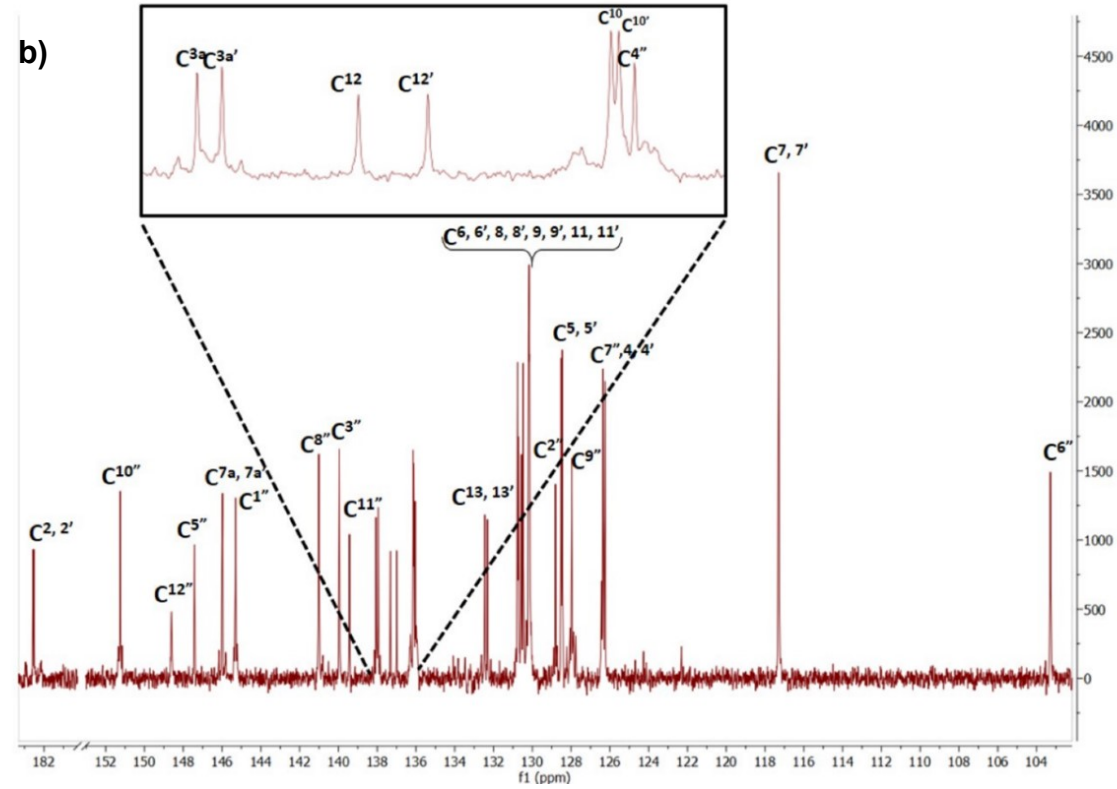
b)
C3a
C3a'
C12
C12'
C10
C10'
C4''
C7, 7'
C6, 6', 8, 8', 9, 9', 11, 11'
C5, 5'
C7'',4,4'
C2''
C9''
C6''
C8''
C3''
C11''
C13, 13'
C10''
C7a, 7a'
C1''
C5''
C2, 2'
C12''
f1 (ppm)

Figure S5. NMR spectra of **6-CF_3CO_2** in CD_3COCD_3 at 298 K a) ^1H, b) $^{13}C\{^1H\}$, c) $^{19}F\{^1H\}$

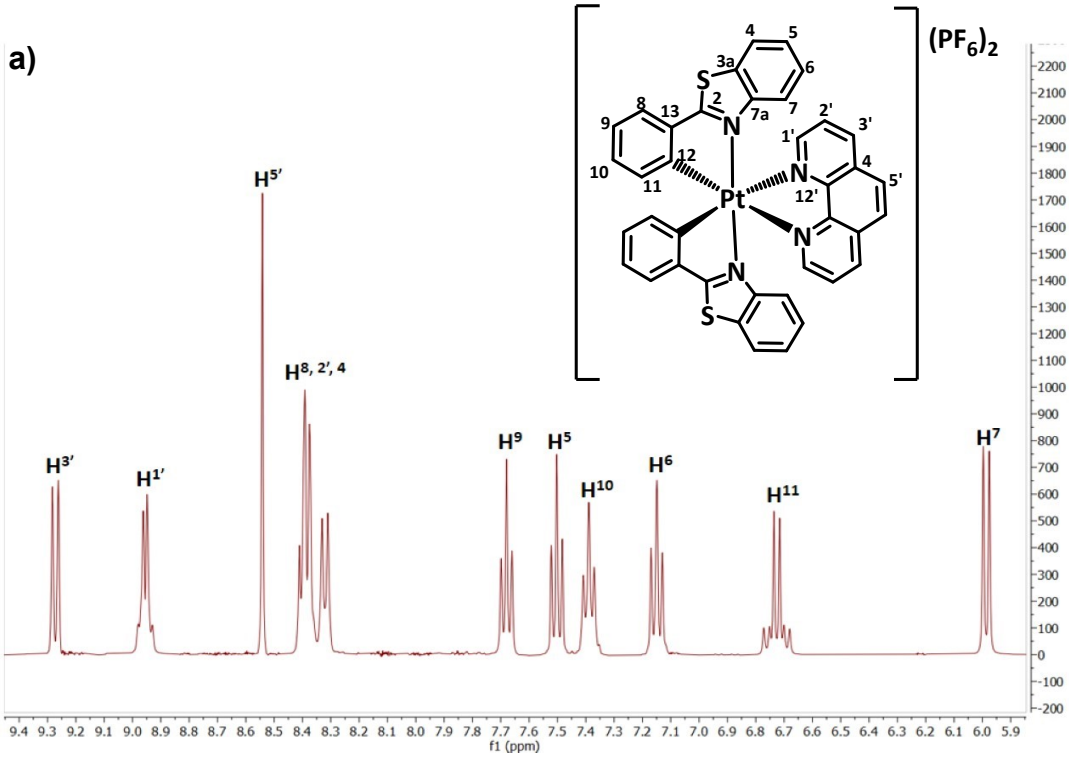
a)
(PF6)2
H3'
H1'
H5'
H8, 2', 4
H9
H5
H10
H6
H11
H7
f1 (ppm)

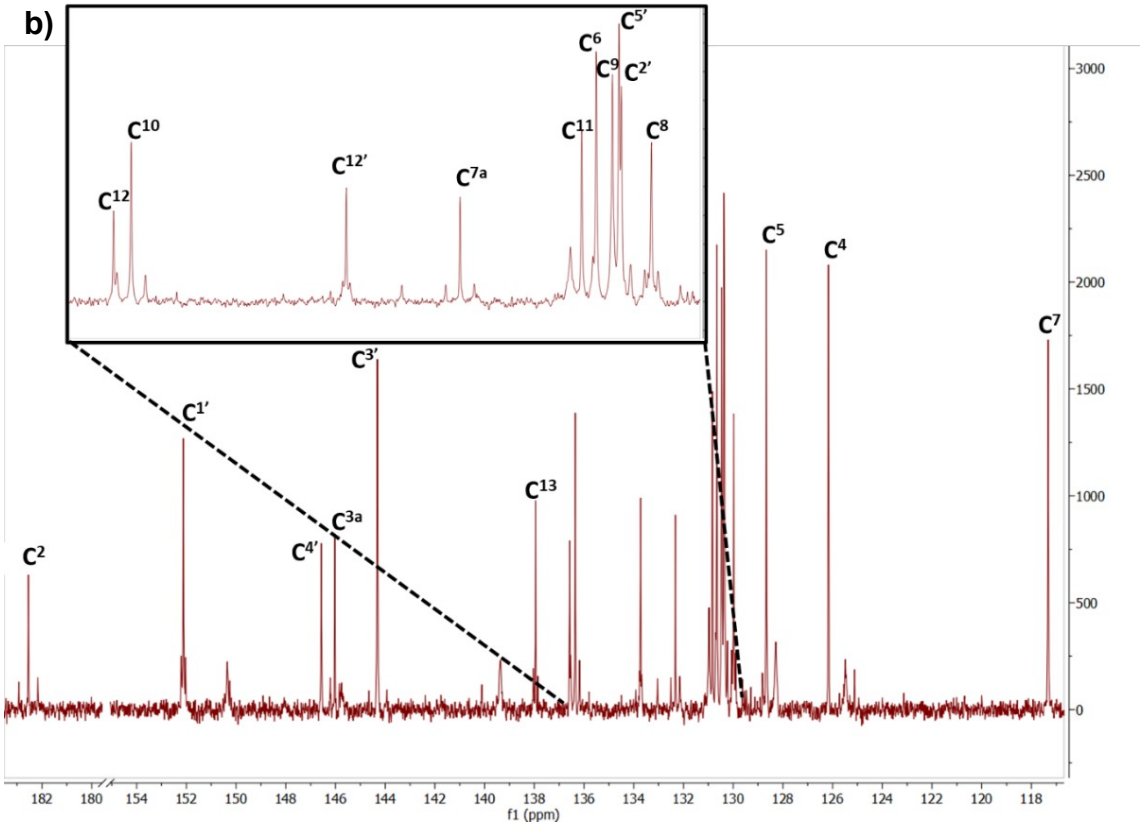
b)
C10
C12
C12'
C7a
C11
C6
C9
C5'
C2'
C8
C5
C4
C7
C3'
C1'
C13
C3a
C4'
C2
f1 (ppm)

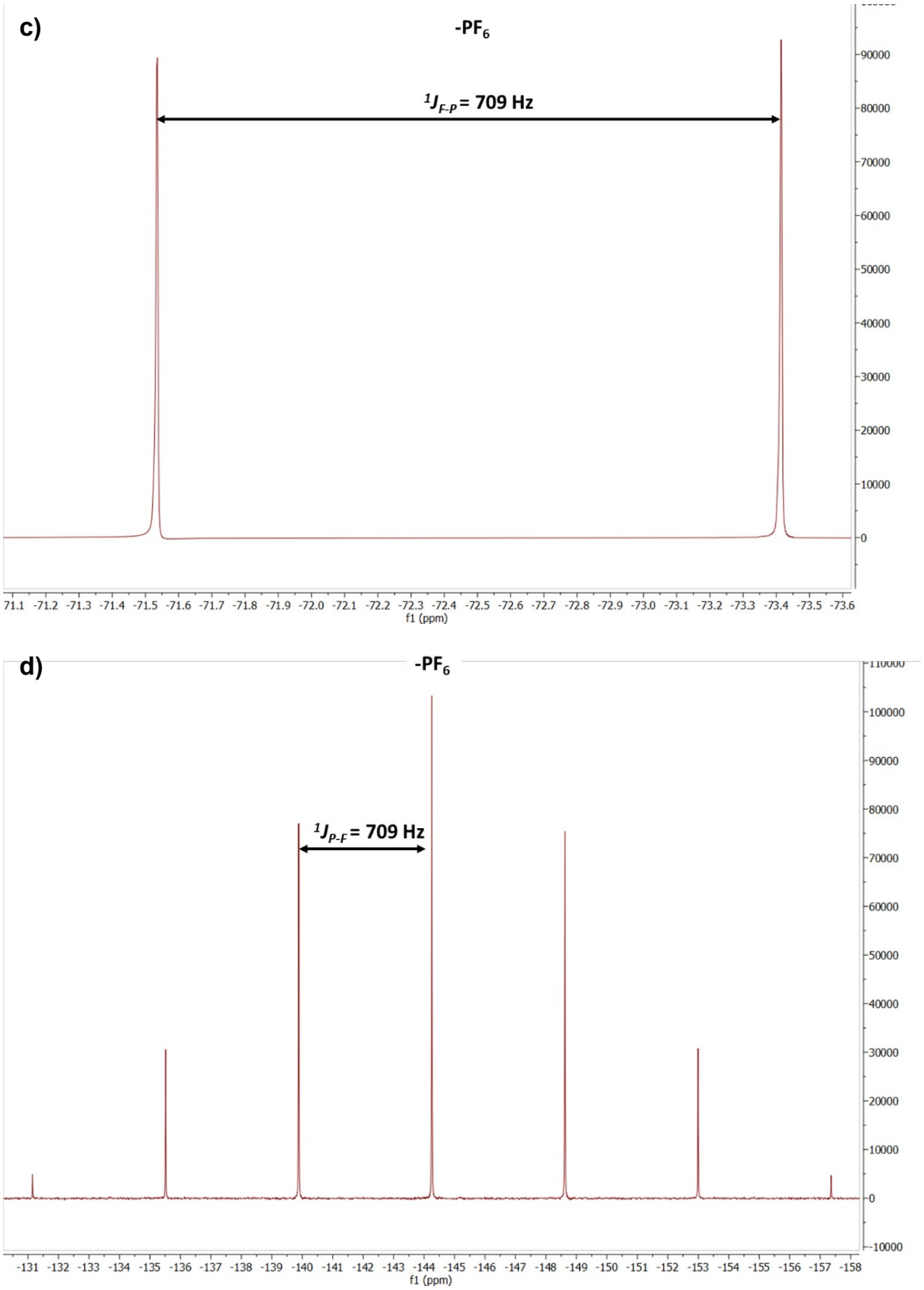

Figure S6. NMR spectra of **4-PF$_6$** in CD_3COCD_3 at 298 K a) ^{1}H, b) ^{13}C{^{1}H}, c) ^{19}F{^{1}H}, d) ^{31}P{^{1}H}

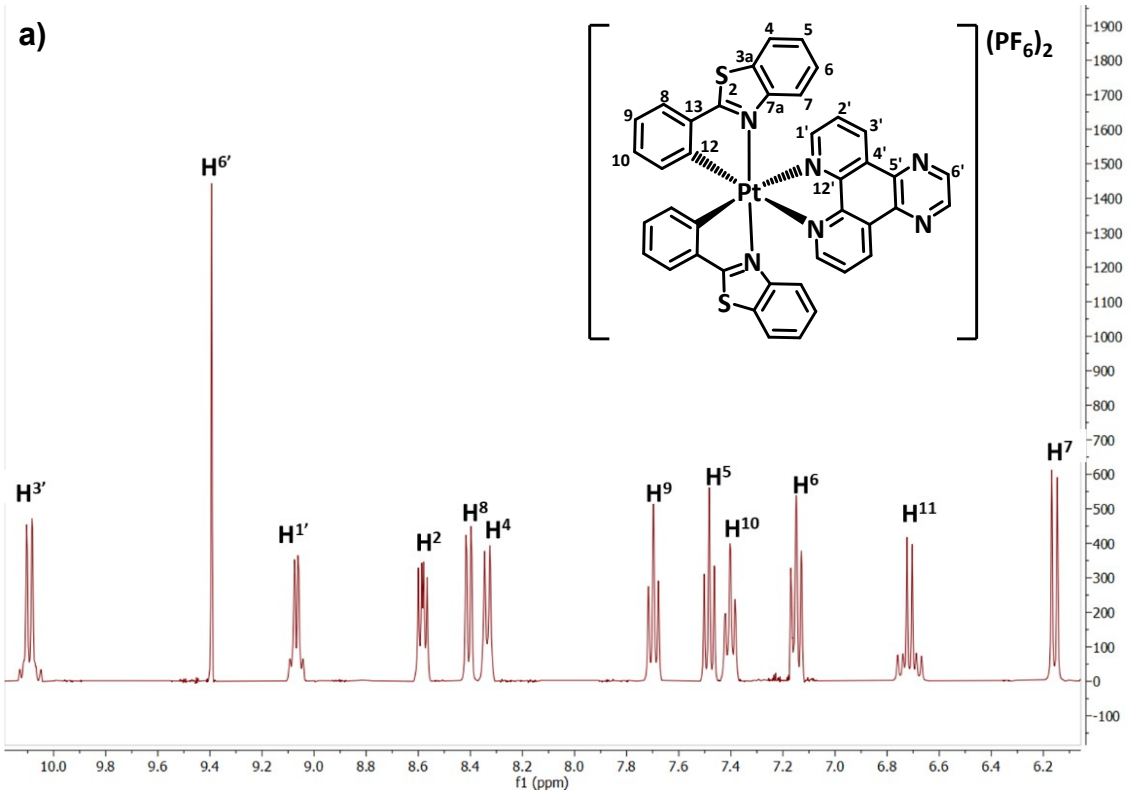
a)
(PF6)2
H6'
H3'
H1'
H2
H8
H4
H9
H5
H10
H6
H11
H7
f1 (ppm)

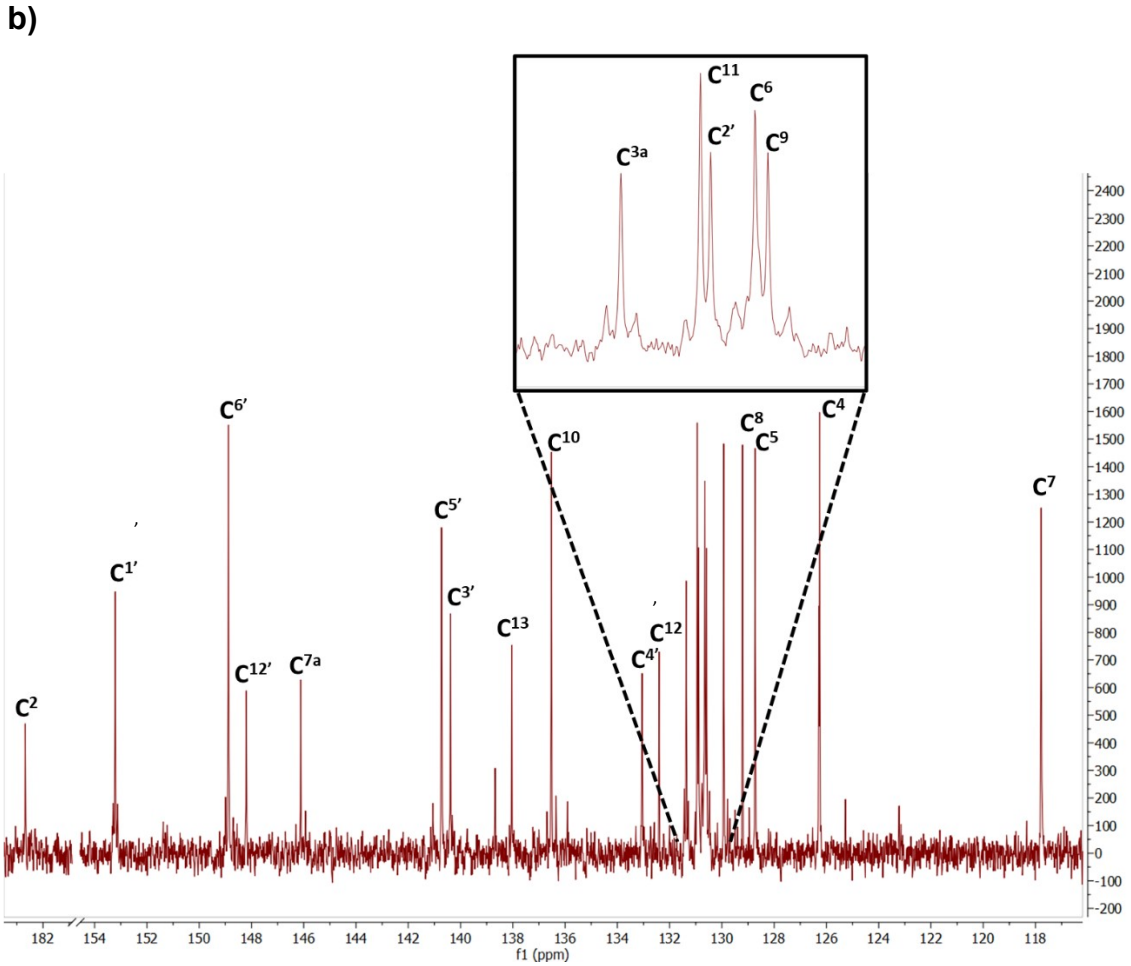
b)
C11
C6
C2'
C9
C3a
C6'
C10
C8
C5
C4
C7
C5'
C1'
C3'
C13
C12
C4'
C12'
C7a
C2
f1 (ppm)

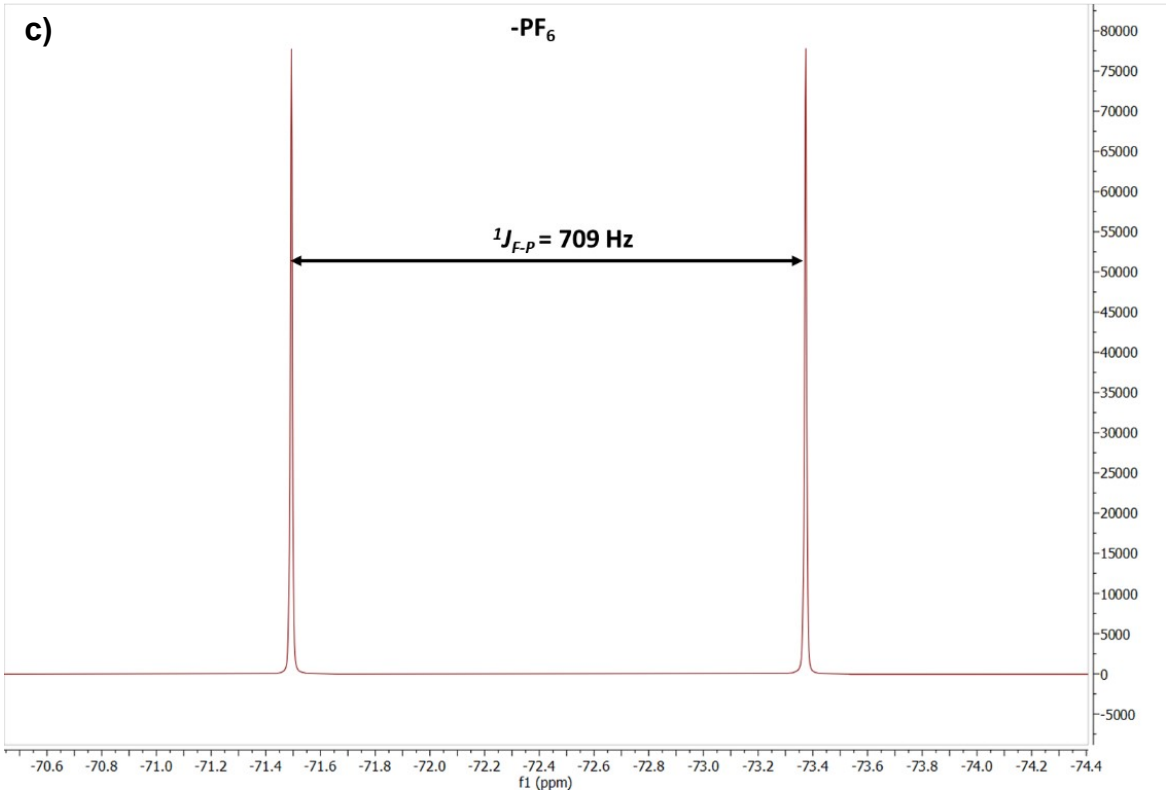

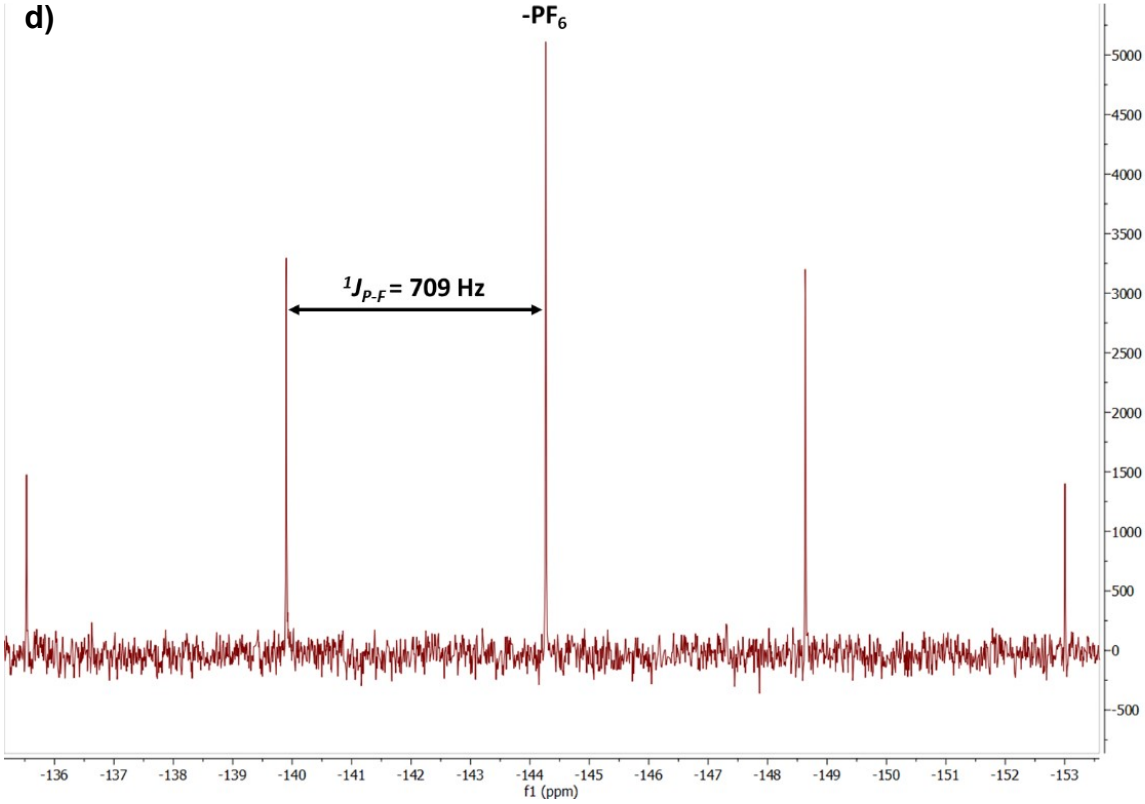

Figure S7. NMR spectra of **5-PF$_6$** in CD_3COCD_3 at 298 K a) ^{1}H, b) ^{13}C{^{1}H}, c) ^{19}F{^{1}H}, d) ^{31}P{^{1}H}

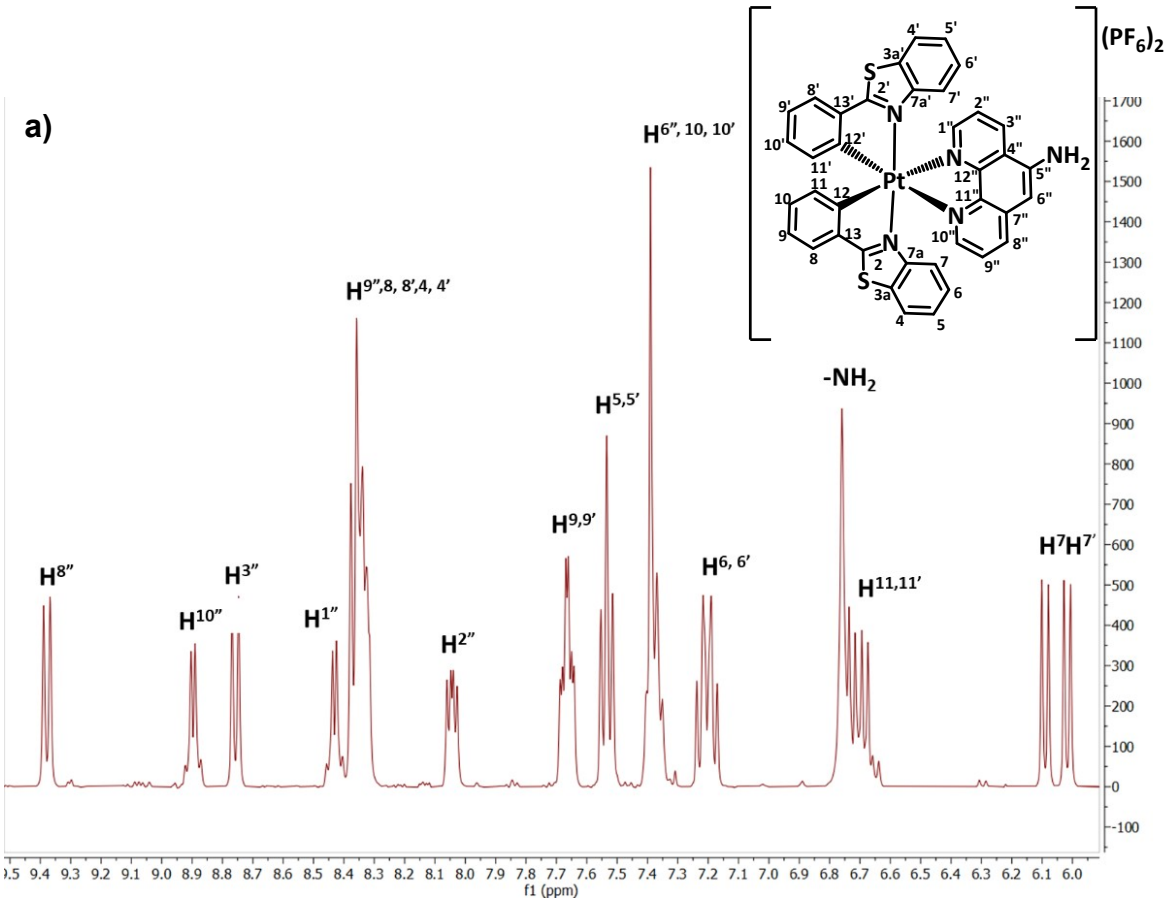
a)
H8”
H10”
H3”
H1”
H9”,8, 8’,4, 4’
H2”
H9,9’
H5,5’
H6”, 10, 10’
H6, 6’
-NH2
H11,11’
H7H7’
(PF6)2
NH2
Pt
f1 (ppm)

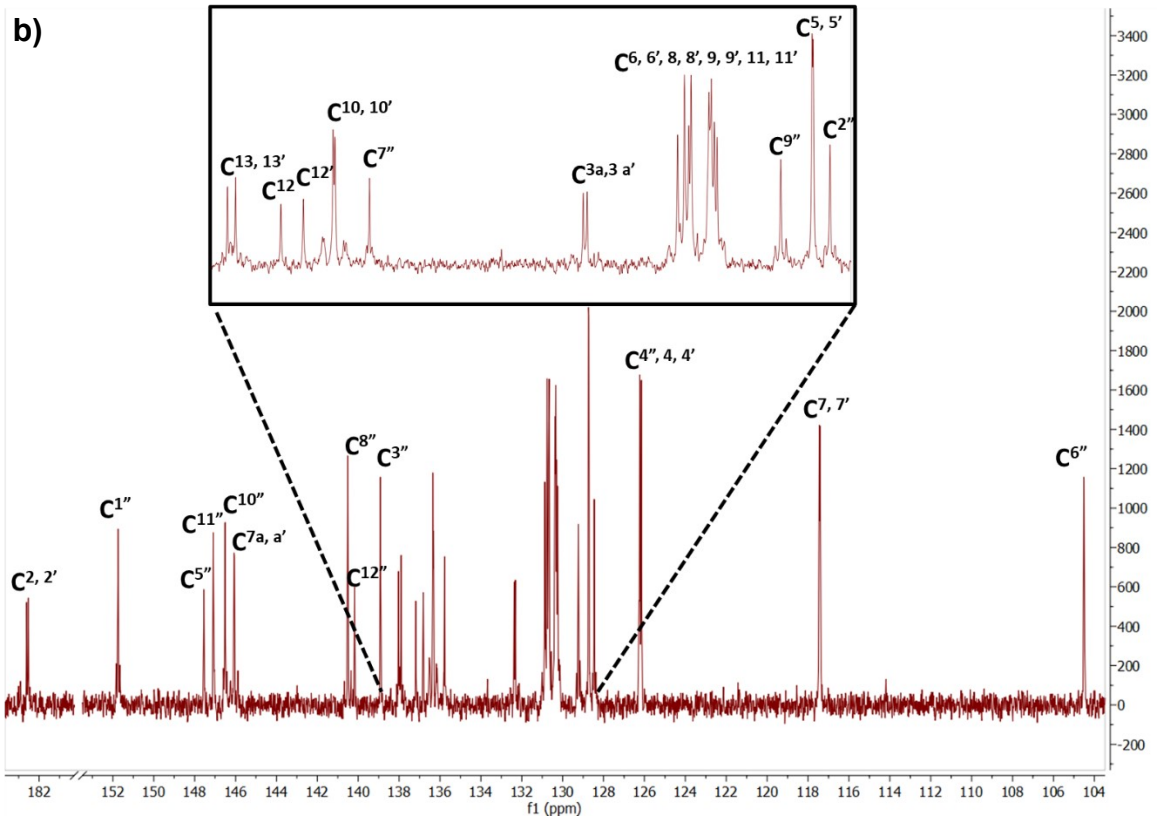
b)
C13, 13’
C12
C12’
C10, 10’
C7”
C3a,3 a’
C6, 6’, 8, 8’, 9, 9’, 11, 11’
C9”
C5, 5’
C2”
C4”, 4, 4’
C7, 7’
C6”
C8”
C3”
C12”
C1”
C11”
C10”
C7a, a’
C5”
C2, 2’
f1 (ppm)

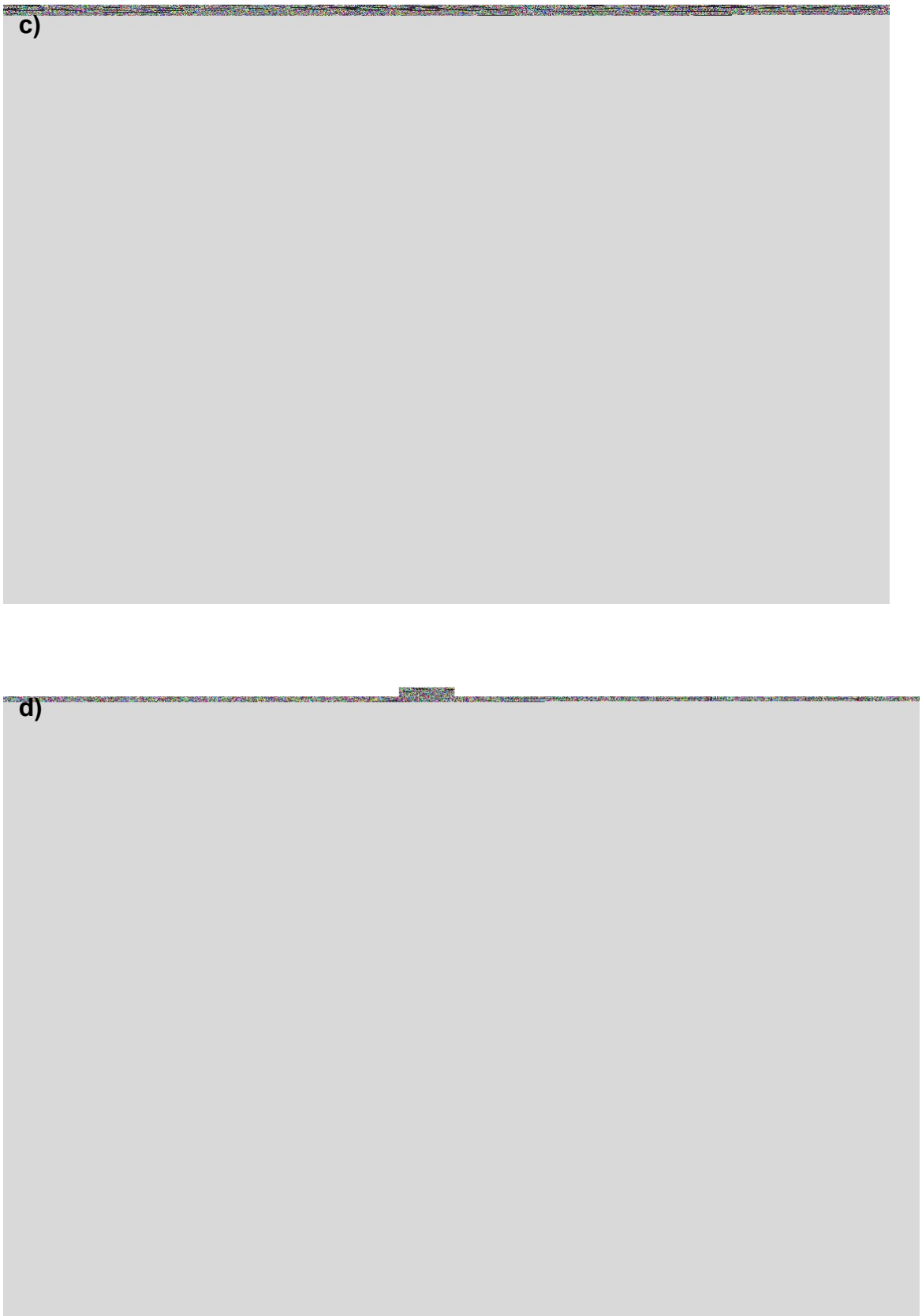

Figure S8. NMR spectra of **6-PF$_6$** in CD_3COCD_3 at 298 K a) ^{1}H, b) ^{13}C{^{1}H}, c) ^{19}F{^{1}H}, d) ^{31}P{^{1}H}

3. X-Ray Diffraction Studies

Table S1. X-ray Crystallographic Data for **2**, **3** and **4-PF$_6$**

	2	**3**	**4-PF$_6$**
Empirical formula	$C_{26}H_{16}Cl_2N_2PtS_2$	$C_{30}H_{16}F_6N_2O_4PtS_2$	$C_{38}H_{24}F_{12}N_4P_2PtS_2$
Molecular weight	686.52	841.66	1085.76
T (K)	100(2) K	300(2) K	100(2) K
Wavelength (Å)	0.71076	0.71076	0.71073
Crystal system	Orthorhombic	Monoclinic	Orthorhombic
Space group	P b c a	P 2_1/c	P b c n
Crystal size (mm)	0.119 x 0.070 x 0.053	0.290 x 0.273 x 0.064	0.450 x 0.115 x 0.075
a (Å)	12.5836(6)	19.070(4)	14.0515(15)
b (Å)	14.5133(7)	17.181(4)	15.0725(15)
c (Å)	24.9740(11)	9.1111(19)	17.2359(19)
α (°)	90	90	90
β (°)	90	91.00	90
γ (°)	90	90	90
V (Å^3)	4561.0(4)	2984.8(11)	3650.4(7)
Z	8	4	4
Density (calculated) (Mg/cm^3)	2.000	1.873	1.976
Absorption coefficient (mm^{-1})	6.589	4.918	4.146
F(000)	2640	1624	2112
θ range for data collection (°)	2.693 to 26.373	3.192 to 28.043	3.085 to 25.677
Index ranges	-15<=h<=15, -18<=k<=18, -31<=l<=31	-25<=h<=25, -22<=k<=22, -11<=l<=11	17<=h<=17, -18<=k<=18, -20<=l<=20
Reflections collected	257759	139304	119953
Independent reflections	4655 [R(int) = 0.0311]	7077 [R(int) = 0.0393]	2715 [R(int) = 0.0278]
Data / restraints / parameters	4655 / 0 / 298	7077 / 0 / 406	2715 / 0 / 267
Goodness-of-fit on F2	1.099	1.113	1.249
Final R indices [I>2σ(I)][a]	R1 = 0.0150, wR2 = 0.0347	R1 = 0.0246, wR2 = 0.0540	R1 = 0.0278, wR2 = 0.0602
R indices (all data)[a]	R1 = 0.0156, wR2 = 0.0351	R1 = 0.0314, wR2 = 0.0585	R1 = 0.0295, wR2 = 0.0605
Largest diff. peak and hole (e Å^{-3}) (dmin/dmax)	2.048 and -0.899	0.725 and -0.804	1.342 and -0.667

[a] $R1 = \Sigma(|F_o| - |F_c|)/\Sigma|F_o|$; $wR2 = [\Sigma w(F_o^2 - F_c^2)^2/\Sigma wF_o^2]^{1/2}$; goodness of fit = $\{\Sigma[w(F_o^2 - F_c^2)^2]/(N_{obs} - N_{param})\}^{1/2}$; $w = [\sigma^2(F_o) + (g_1P)^2 + g_2P]^{-1}$; $P = [\max(F_o^2;0 + 2F_c^2]/3$.

Table S2. Selected distances (Å) and angles (º) for complexes **2**, **3** and **4-PF$_6$**

2			
Distances (Å)		**Angles (°)**	
Pt(1)-C(1)	2.025 (2)	C(1)-Pt(1)-N(2)	91.11 (8)
Pt(1)-N(1)	2.0491 (2)	C(1)-Pt(1)-N(1)	81.14 (9)
Pt(1)-C(14)	2.022 (2)	C(1)-Pt(1)-C(14)	90.80 (9)
Pt(1)-N(2)	2.0386 (2)	C(14)-Pt(1)-N(2)	81.00 (9)
Pt(1)-Cl(1)	2.4439 (6)	C(14)-Pt(1)-N(1)	93.76 (9)
Pt(1)-Cl(2)	2.4418 (6)	C(1)-Pt(1)-Cl(2)	90.91 (7)
		N(2)-Pt(1)-Cl(2)	102.52 (6)
		N(1)-Pt(1)-Cl(2)	82.99 (6)
		C(14)-Pt(1)-Cl(1)	87.94 (6)
		N(2)-Pt(1)-Cl(1)	85.53 (6)
		N(1)-Pt(1)-Cl(1)	102.14 (6)
		Cl(2)-Pt(1)-Cl(1)	90.55 (2)
3			
Distances (Å)		**Angles (°)**	
Pt(1)-C(1)	2.013 (3)	C(1)-Pt(1)-N(2)	92.05 (12)
Pt(1)-N(1)	2.031 (2)	C(1)-Pt(1)-N(1)	81.83 (12)
Pt(1)-C(14)	2.031 (4)	C(1)-Pt(1)-C(14)	87.11 (13)
Pt(1)-N(2)	2.029 (3)	N(2)-Pt(1)-C(14)	80.57 (15)
Pt(1)-O(1)	2.133 (2)	N(1)-Pt(1)-C(14)	95.25 (13)
Pt(1)-O(3)	2.158 (3)	N(2)-Pt(1)-O(1)	92.04 (9)
		N(1)-Pt(1)-O(1)	94.04(10)
		C(14)-Pt(1)-O(1)	92.92(12)
		C(1)-Pt(1)-O(3)	98.25(12)
		N(2)-Pt(1)-O(3)	98.11(11)
		N(1)-Pt(1)-O(3)	86.60(10)
		O(1)-Pt(1)-O(3)	81.81(10)
4-PF$_6$			
Distances (Å)		**Angles (°)**	
Pt(1)-C(1)	2.021(5)	C(1)-Pt(1)-N(2)	90.94(18)
Pt(1)-N(1)	2.055(4)	C(1)-Pt(1)-N(1)	81.31(18)
Pt(1)-C(14)	2.021(5)	C(1)-Pt(1)-C(14)	85.8(3)
Pt(1)-N(2)	2.055(4)	C(14)-Pt(1)-N(2)	81.31(18)
Pt(1)-N(3)	2.126(4)	C(14)-Pt(1)-N(1)	90.94(18)
Pt(1)-N(4)	2.126(4)	C(14)-Pt(1)-N(4)	97.64(17)
		N(1)-Pt(1)-N(4)	97.66(15)
		N(2)-Pt(1)-N(4)	90.51(15)
		C(1)-Pt(1)-N(3)	97.64(17)
		N(1)-Pt(1)-N(3)	90.51(15)
		N(2)-Pt(1)-N(3)	97.66(15)
		N(4)-Pt(1)-N(3)	78.9(2)

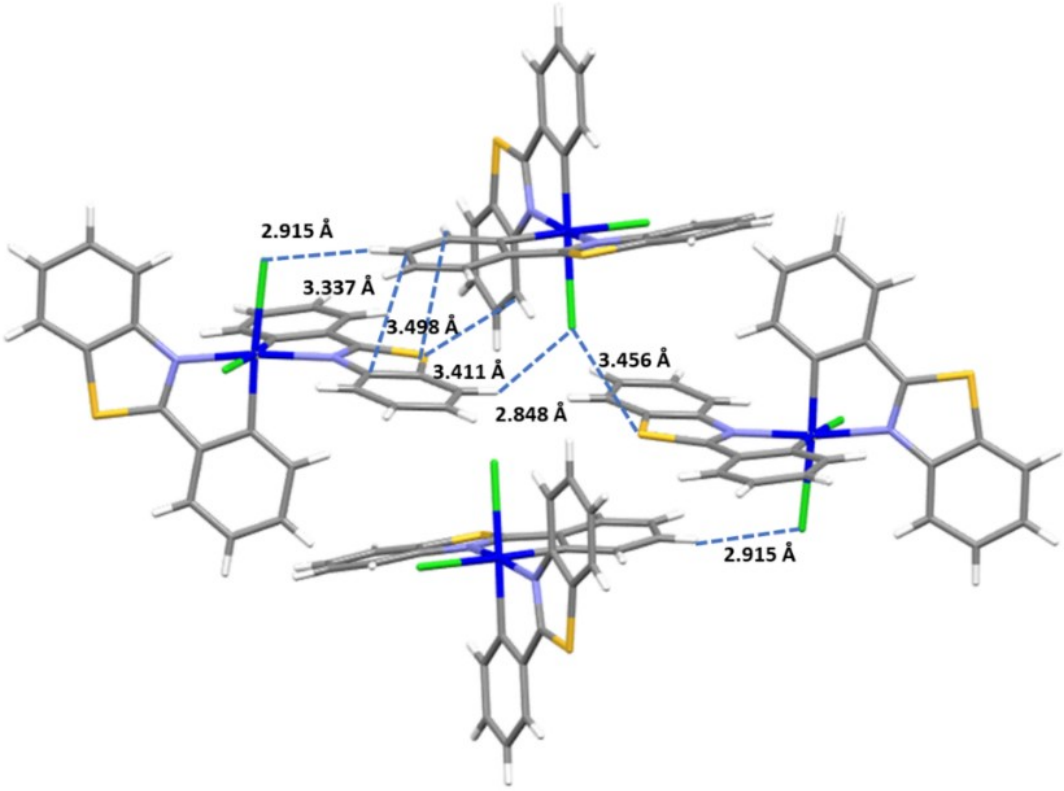

Figure S9. Crystal Packing of **2** showing some intermolecular contacts

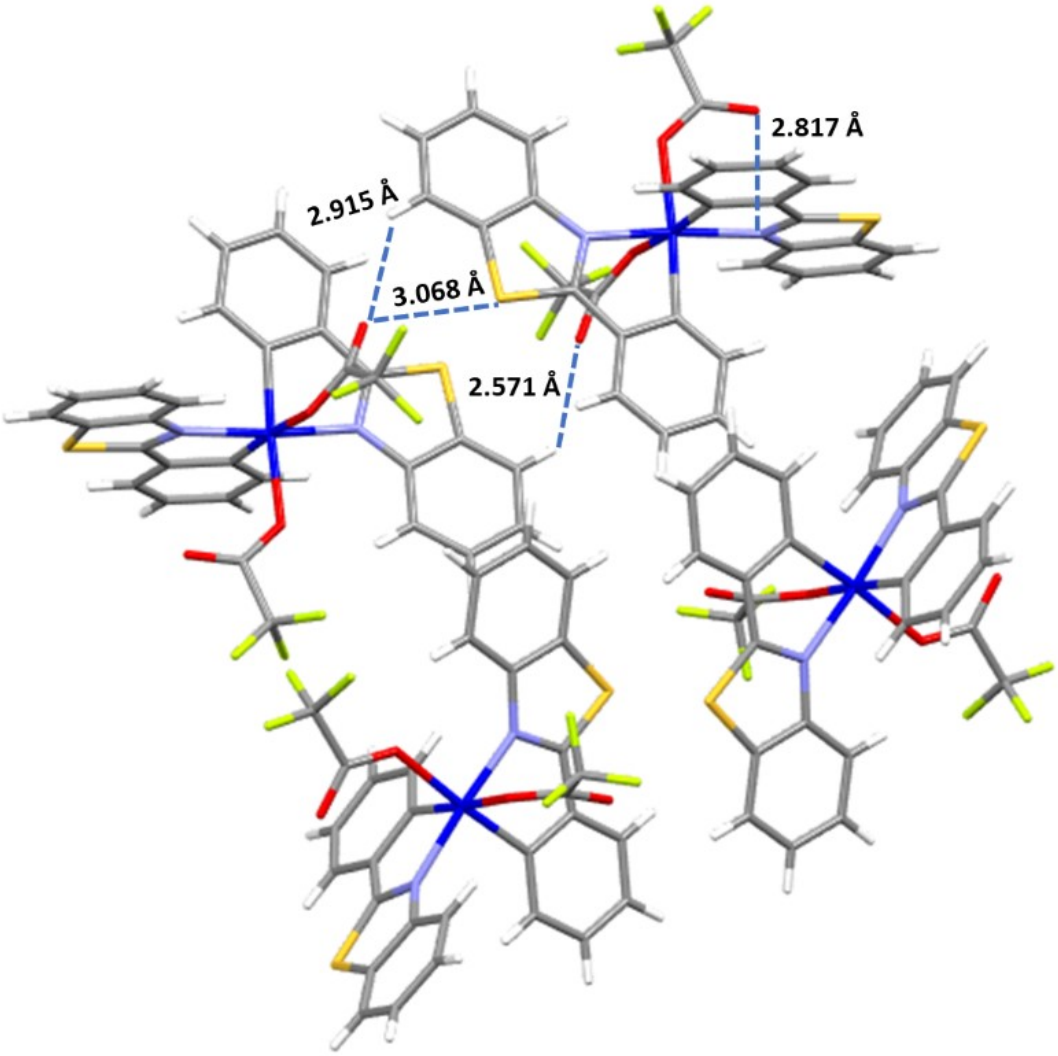

Figure S10. Crystal Packing of **3** showing some intermolecular contacts

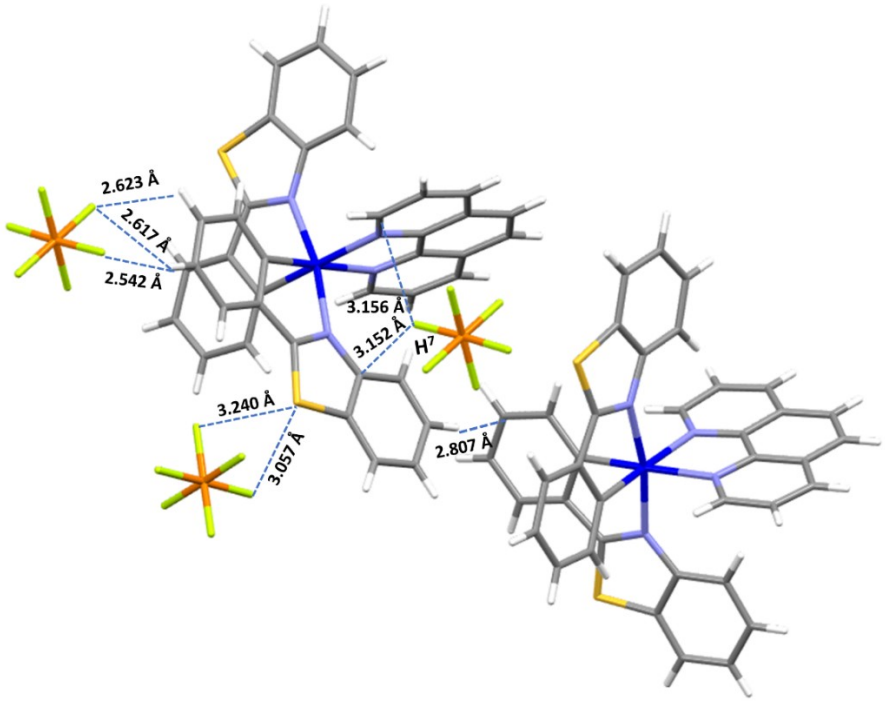

Figure S11. Crystal Packing of **4-PF$_6$** showing some intermolecular contacts

4. Photophysical Properties and Theoretical Calculations

Table S3. UV-Vis absorption data in CH_2Cl_2 solution (5 x 10^{-5} M)	
Complex	**λ /nm (ε x 10^{-3} / mol^{-1}·L·cm^{-1})**
[Pt(pbt)Cl(Hpbt-*κN*)] **1**	254 (23.74), 270 (21.05), 306 (21.40), 335 (12.69), 367 (4.02), 407 (2.87), 425 (2.62)
$[Pt(pbt)_2Cl_2]$ **2**	258 (19.52), 316 (20.57), 347 (18.33), 363 (13.55)
$[Pt(pbt)_2(OCOCF_3)_2]$ **3**	256 (17.95), 322 (20.96), 346 (19.31), 366 (11.52)
$[Pt(pbt)_2(phen)](CF_3CO_2)_2$ **4-CF_3CO_2**	264 (31.45), 266 (31.10), 292 (15.62), 321 (18.29), 349 (17.95), 366 (11.10)
$[Pt(pbt)_2(phen)](PF_6)_2$ **4-PF_6**	261 (37.45), 304 (17.66), 345 (12.80), 367 (2.35)
$[Pt(pbt)_2(pyraphen)](CF_3CO_2)_2$ **5-CF_3CO_2**	257 (66.03), 307 (27.40), 341 (25.42), 367 (13.22)
$[Pt(pbt)_2(pyraphen)](PF_6)_2$ **5-PF_6**	270 (20.17), 277 (19.50), 304 (7.76), 350 (7.64), 367 (4.80)
$[Pt(pbt)_2(NH_2\text{-phen})](CF_3CO_2)_2$ **6-CF_3CO_2**	252 (33.25), 266 (27.24), 276 (21.58), 310 (30.68), 348 (24.11), 366 (18.02), 400 (4.85), 480 (1.10)
$[Pt(pbt)_2(NH_2\text{-phen})](PF_6)_2$ **6-PF_6**	250 (18.15), 266 (15.64), 306 (21.21), 350 (14.76), 367 (10.59), 389 (2.20), 443 (0.83)

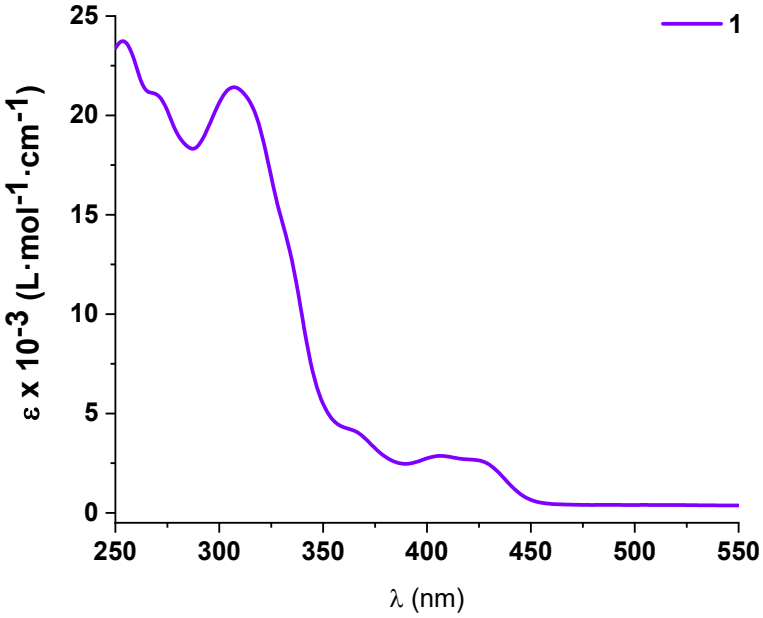

Figure S12. UV-Vis absorption spectra for complex **1** in CH_2Cl_2 solution (5 x 10^{-5} M) at 298 K

Table S4. DFT optimized geometries for ground state and triplet state (in CH_2Cl_2)

2			
S_0		*T_1*	
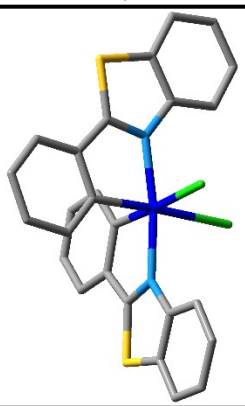		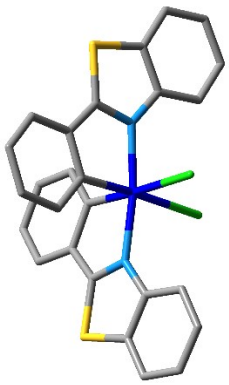	
	X-Ray	*S_0*	*T_1*
Pt(1)-C(1)	2.025 (2)	2.0385	2.0385
Pt(1)-N(1)	2.0491 (2)	2.0882	2.0882
Pt(1)-C(14)	2.022 (2)	2.0384	2.0384
Pt(1)-N(2)	2.0386 (2)	2.0883	2.0883
Pt(1)-Cl(1)	2.4439 (6)	2.5440	2.5440
Pt(1)-Cl(2)	2.4418 (6)	2.5452	2.5452
C(1)-Pt(1)-N(2)	91.11 (8)	93.6235	93.5908
C(1)-Pt(1)-N(1)	81.14 (9)	80.4590	80.4567
C(1)-Pt(1)-C(14)	90.80 (9)	89.9957	89.9956
C(14)-Pt(1)-N(2)	81.00 (9)	80.4567	80.4590
C(14)-Pt(1)-N(1)	93.76 (9)	93.5908	93.6235
C(1)-Pt(1)-Cl(2)	90.91 (7)	89.2451	89.5442
N(2)-Pt(1)-Cl(2)	102.52 (6)	102.0679	102.1023
N(1)-Pt(1)-Cl(2)	82.99 (6)	83.8360	83.7980
C(14)-Pt(1)-Cl(1)	87.94 (6)	89.5443	89.2451
N(2)-Pt(1)-Cl(1)	85.53 (6)	83.7980	83.8360
N(1)-Pt(1)-Cl(1)	102.14 (6)	102.1023	102.0679
Cl(2)-Pt(1)-Cl(1)	90.55 (2)	91.3237	91.3237

3			
S_0		*T_1*	
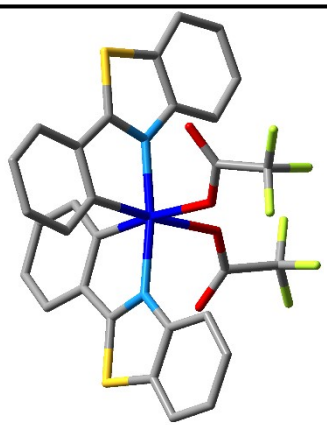		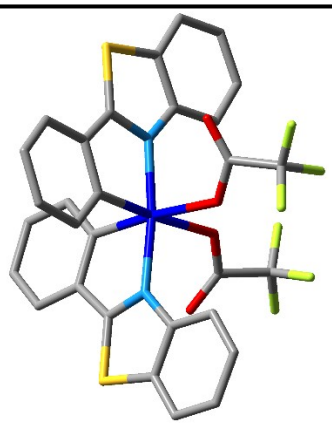	
	X-Ray	*S_0*	*T_1*
Pt(1)-C(1)	2.013 (3)	2.0297	2.0261
Pt(1)-N(1)	2.031 (2)	2.0780	2.0863
Pt(1)-C(14)	2.031 (4)	2.0297	2.0346
Pt(1)-N(2)	2.029 (3)	2.0779	2.0569
Pt(1)-O(1)	2.133 (2)	2.1956	2.2087
Pt(1)-O(3)	2.158 (3)	2.1956	2.2188
C(1)-Pt(1)-N(2)	92.05 (12)	93.6317	93.9035
C(1)-Pt(1)-N(1)	81.83 (12)	80.7604	80.6942
C(1)-Pt(1)-C(14)	87.11 (13)	88.0882	87.8366
N(2)-Pt(1)-C(14)	80.57 (15)	80.7596	81.6712
N(1)-Pt(1)-C(14)	95.25 (13)	93.6355	93.7166
N(2)-Pt(1)-O(1)	92.04 (9)	90.3444	90.3743
N(1)-Pt(1)-O(1)	94.04(10)	95.5724	95.2599
C(14)-Pt(1)-O(1)	92.92(12)	95.7405	95.7584
C(1)-Pt(1)-O(3)	98.25(12)	95.7442	96.0490
N(2)-Pt(1)-O(3)	98.11(11)	95.5733	95.5733
N(1)-Pt(1)-O(3)	86.60(10)	90.3410	90.4192
O(1)-Pt(1)-O(3)	81.81(10)	80.6439	80.6080

4^{2+}			
S_0		*T_1*	
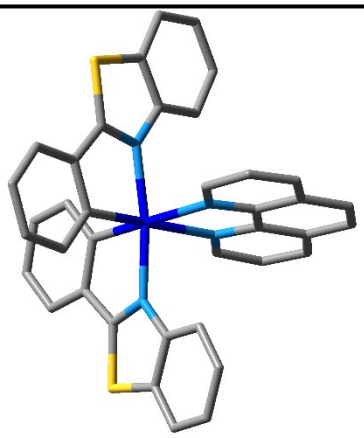		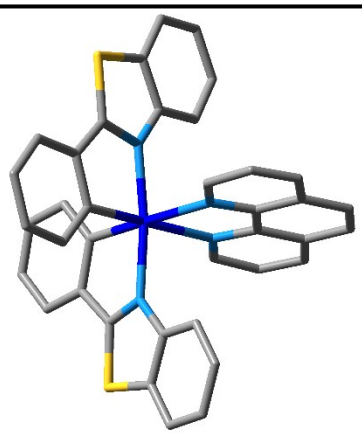	
	X-Ray	*S_0*	*T_1*
Pt(1)-C(1)	2.021(5)	2.0372	2.0374
Pt(1)-N(1)	2.055(4)	2.0899	2.0882
Pt(1)-C(14)	2.021(5)	2.0377	2.0381
Pt(1)-N(2)	2.055(4)	2.0884	2.0871
Pt(1)-N(3)	2.126(4)	2.2392	2.2384
Pt(1)-N(4)	2.126(4)	2.2374	2.2373
C(1)-Pt(1)-N(2)	90.94(18)	93.7396	93.7900
C(1)-Pt(1)-N(1)	81.31(18)	80.5000	80.5300
C(1)-Pt(1)-C(14)	85.8(3)	88.9888	88.7632
C(14)-Pt(1)-N(2)	81.31(18)	80.5224	80.5380
C(14)-Pt(1)-N(1)	90.94(18)	93.7475	93.8107
C(14)-Pt(1)-N(4)	97.64(17)	-	-
N(1)-Pt(1)-N(4)	97.66(15)	85.2987	85.4532
N(2)-Pt(1)-N(4)	90.51(15)	101.0633	100.8311
C(1)-Pt(1)-N(3)	97.64(17)	-	-
N(1)-Pt(1)-N(3)	90.51(15)	100.8999	100.6109
N(2)-Pt(1)-N(3)	97.66(15)	85.4947	85.7075
N(4)-Pt(1)-N(3)	78.9(2)	75.6670	75.0290

5^{2+}			
S_0		*T_1*	
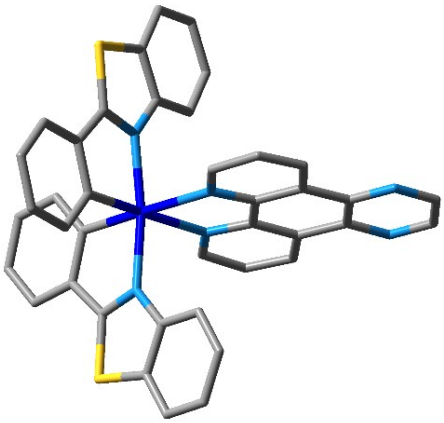		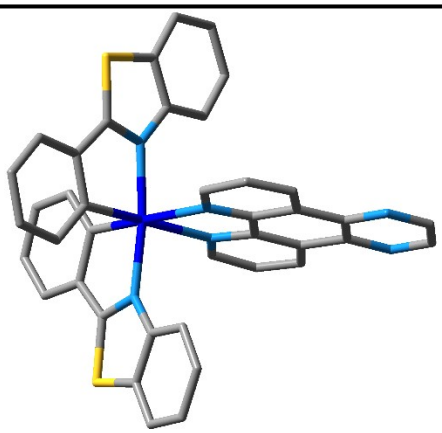	
	X-Ray	*S_0*	*T_1*
Pt(1)-C(1)		2.0372	2.0377
Pt(1)-N(1)		2.0895	2.0897
Pt(1)-C(14)		2.0372	2.0377
Pt(1)-N(2)		2.0895	2.0897
Pt(1)-N(3)		2.2392	2.2291
Pt(1)-N(4)		2.2392	2.2291
C(1)-Pt(1)-N(2)		93.7024	93.6798
C(1)-Pt(1)-N(1)		80.5207	80.4967
C(1)-Pt(1)-C(14)		88.7520	88.8522
C(14)-Pt(1)-N(2)		80.5208	80.4967
C(14)-Pt(1)-N(1)		93.7017	93.6790
C(14)-Pt(1)-N(4)		-	-
N(1)-Pt(1)-N(4)		85.3883	85.4404
N(2)-Pt(1)-N(4)		101.0262	101.0133
C(1)-Pt(1)-N(3)		-	-
N(1)-Pt(1)-N(3)		101.0264	101.0126
N(2)-Pt(1)-N(3)		85.3876	85.4404
N(4)-Pt(1)-N(3)		75.3755	75.7815

6^{2+}			
S_0		*T_1*	
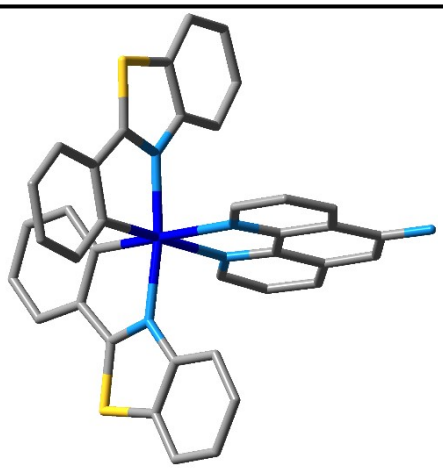		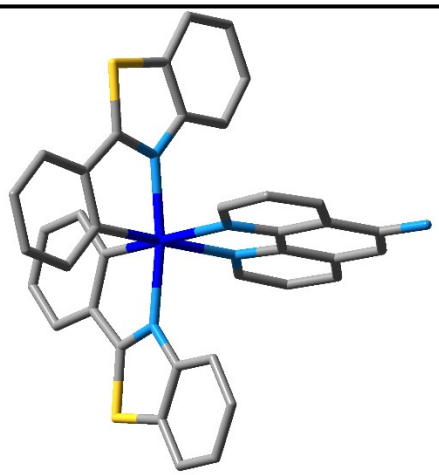	
	X-Ray	*S_0*	*T_1*
Pt(1)-C(1)		2.0386	2.0370
Pt(1)-N(1)		2.0905	2.0905
Pt(1)-C(14)		2.0392	2.0381
Pt(1)-N(2)		2.0889	2.0756
Pt(1)-N(3)		2.2364	2.2507
Pt(1)-N(4)		2.2259	2.2369
C(1)-Pt(1)-N(2)		93.8141	94.2081
C(1)-Pt(1)-N(1)		80.4658	80.4526
C(1)-Pt(1)-C(14)		88.6261	88.7312
C(14)-Pt(1)-N(2)		80.4936	80.3255
C(14)-Pt(1)-N(1)		93.8681	93.6146
C(14)-Pt(1)-N(4)		-	-
N(1)-Pt(1)-N(4)		85.4853	85.5137
N(2)-Pt(1)-N(4)		100.7751	100.2110
C(1)-Pt(1)-N(3)		-	-
N(1)-Pt(1)-N(3)		100.9519	101.0276
N(2)-Pt(1)-N(3)		83.3482	84.7959
N(4)-Pt(1)-N(3)		75.7489	75.3589

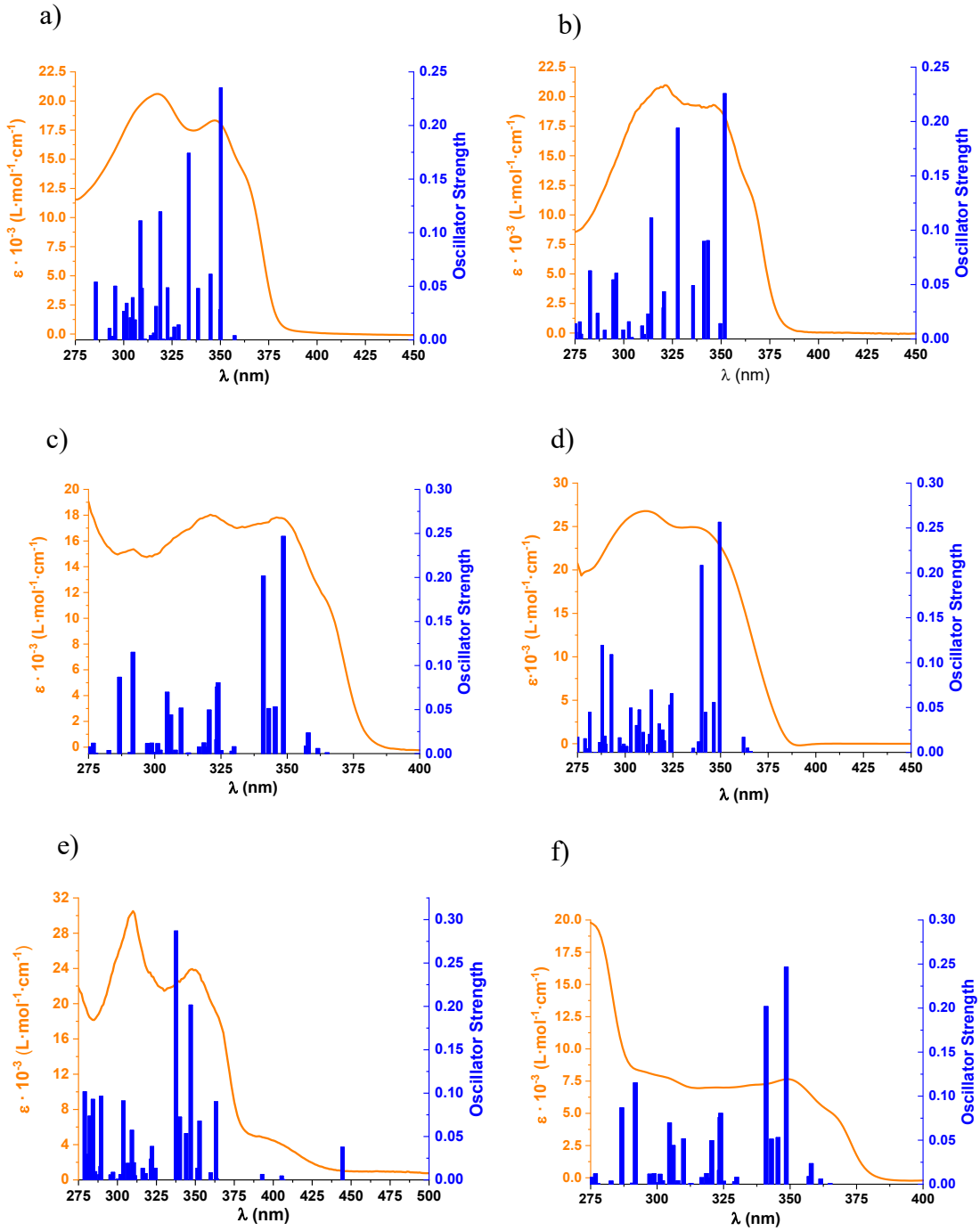
a)
b)
c)
d)
e)
f)
ε · 10⁻³ (L·mol⁻¹·cm⁻¹)
Oscillator Strength
λ (nm)

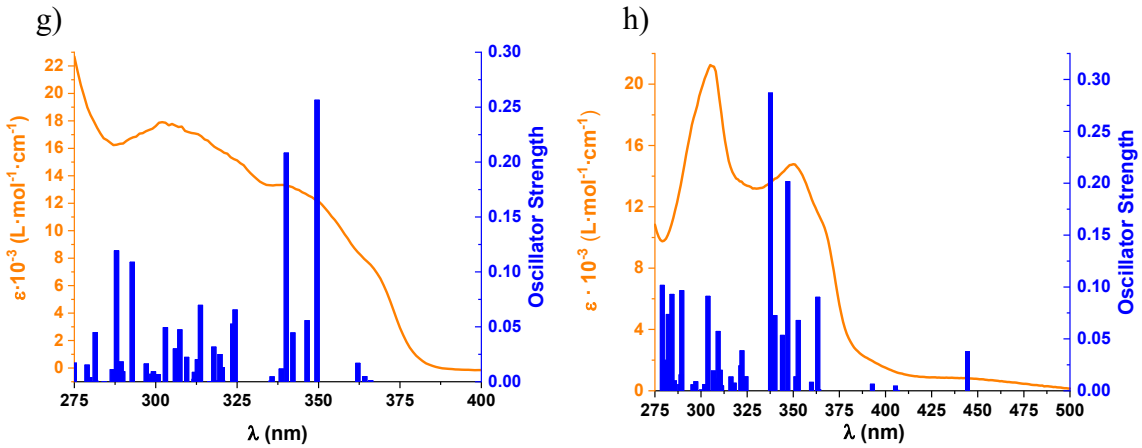

Figure S13. UV-Vis absorption experimental spectra (orange) and calculated transitions (blue) in CH_2Cl_2 for a) **2**, b) **3**, c) **4-CF$_3$CO$_2$**, d) **5-CF$_3$CO$_2$**, e) **6-CF$_3$CO$_2$**, f) **4-PF$_6$**, g) **5-PF$_6$** and h) **6-PF$_6$**

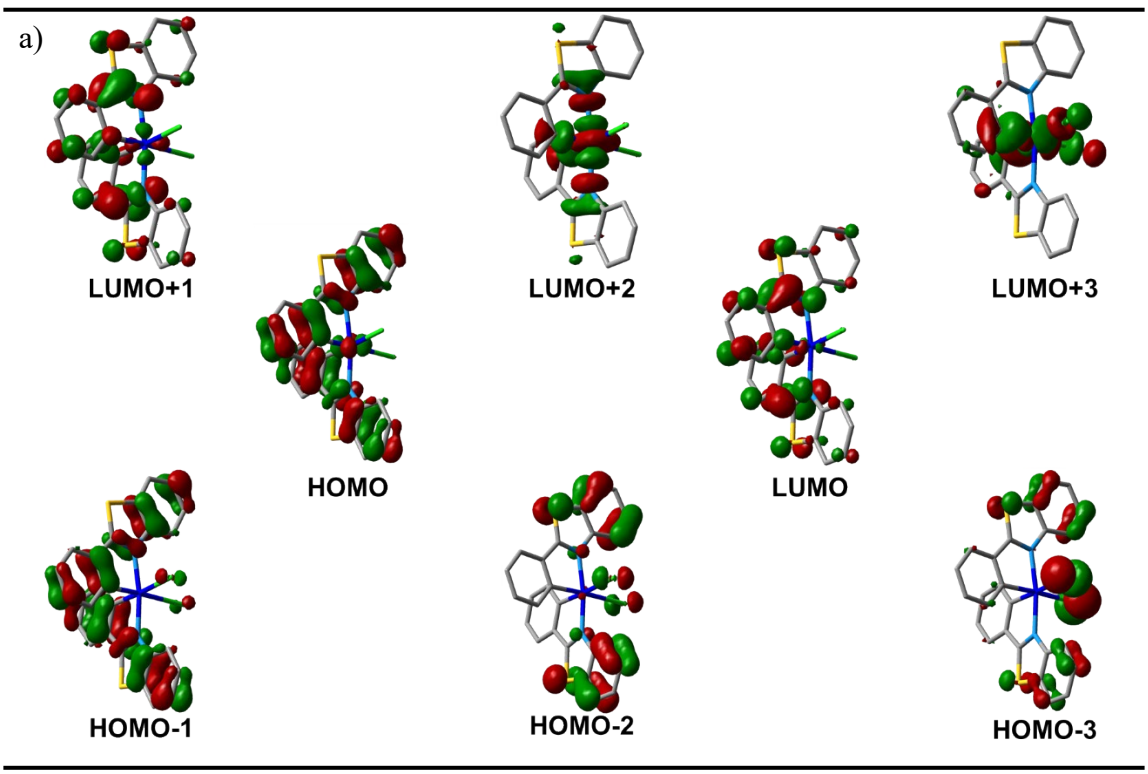

b)

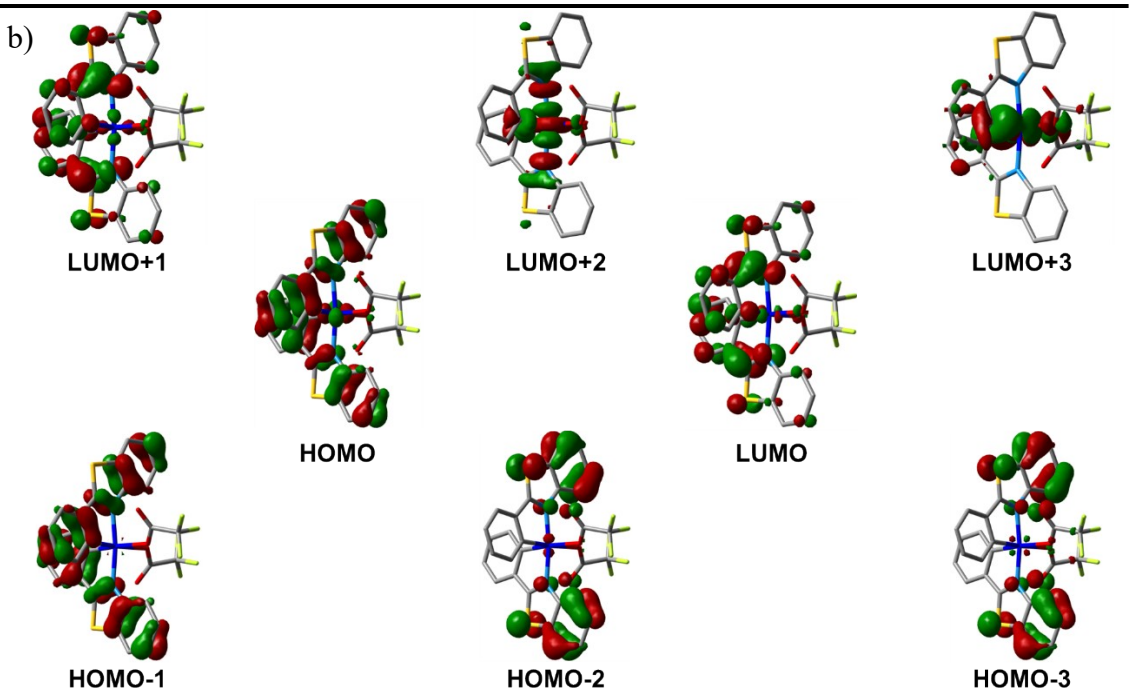
LUMO+1
LUMO+2
LUMO+3
HOMO
LUMO
HOMO-1
HOMO-2
HOMO-3

c)

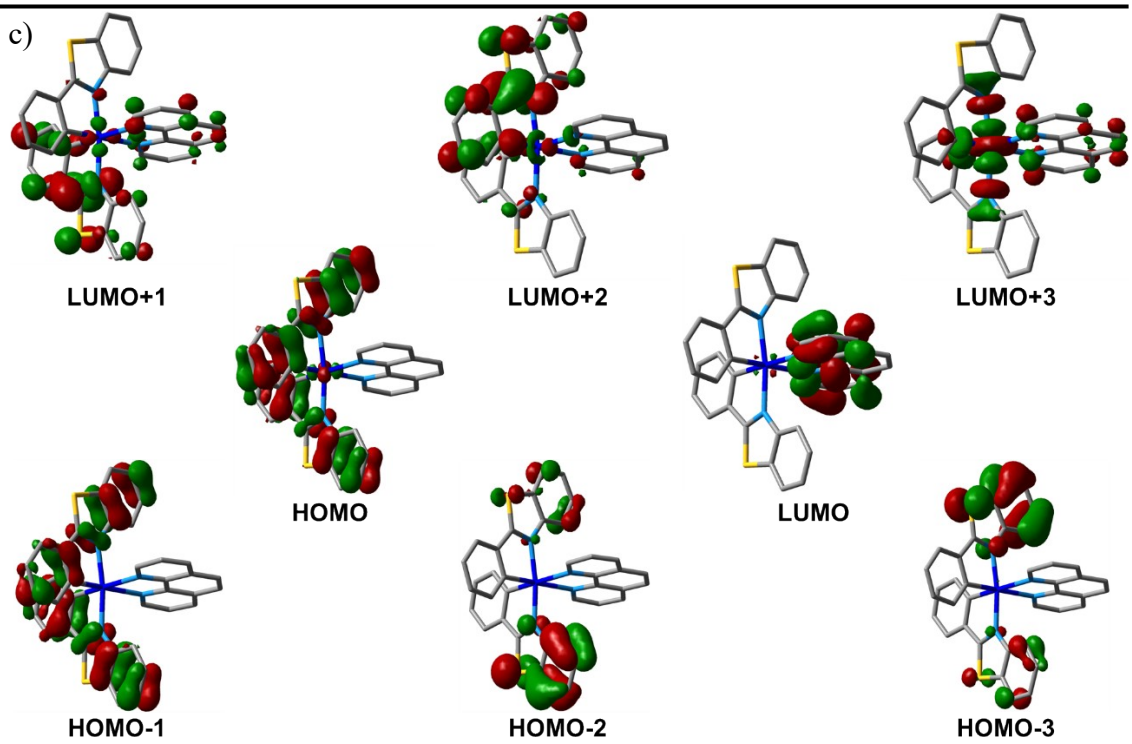
LUMO+1
LUMO+2
LUMO+3
HOMO
LUMO
HOMO-1
HOMO-2
HOMO-3

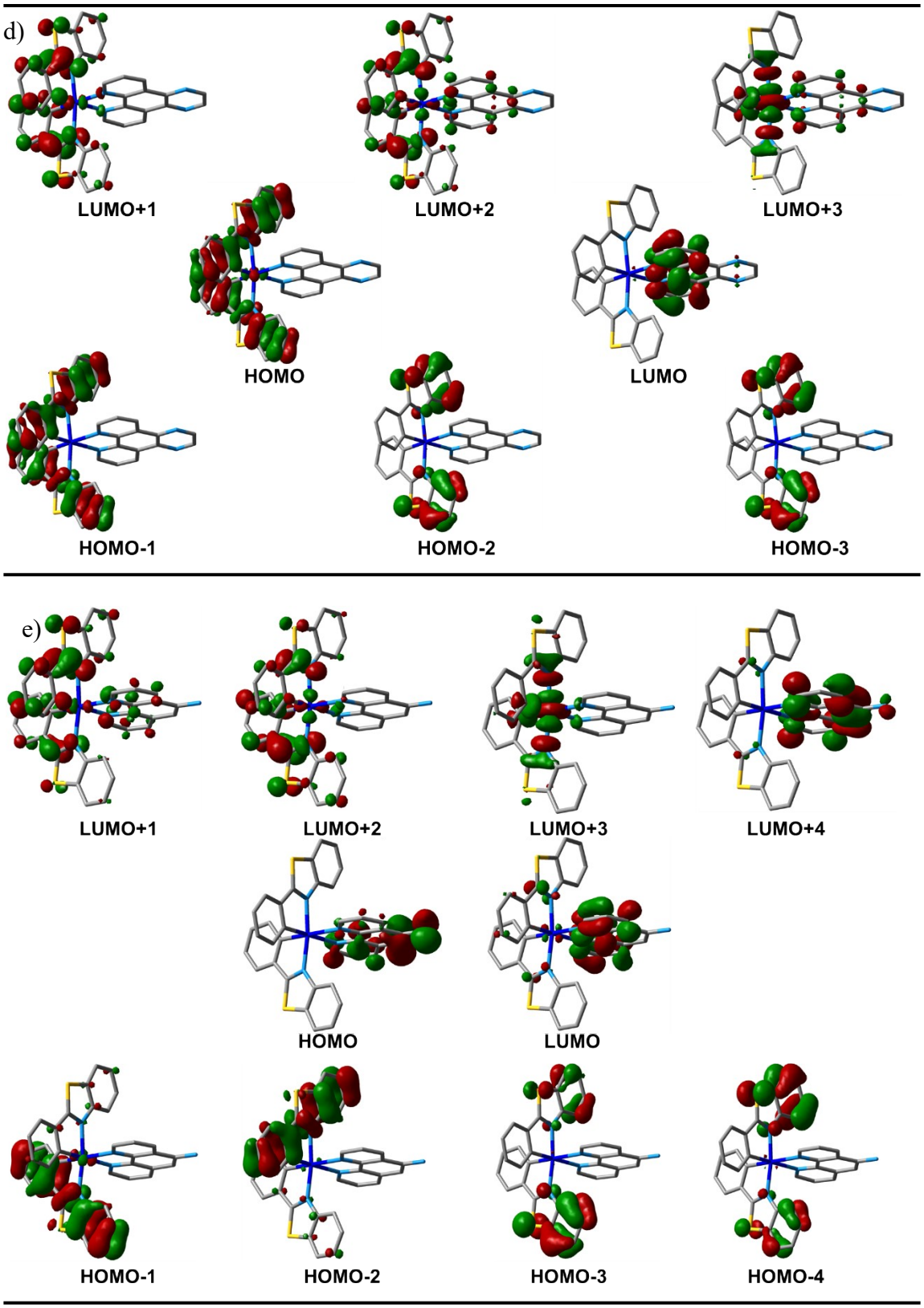

Figure S14. Selected frontier Molecular Orbitals for a) **2**, b) **3**, c) $\mathbf{4}^{2+}$, d) $\mathbf{5}^{2+}$ and e) $\mathbf{6}^{2+}$ in the ground state.

Table S5. Selected vertical excitation energies singlets (S_0) and first triplets computed by TD-DFT/SCRF (CH_2Cl_2) with the orbitals involved.

Complex	State	λ/nm	*f*	Transition (% Contribution)	Character
2	T_1	468.7	-	H-1→L+1 (38%), HOMO→LUMO (45%)	IL
	T_2	468.6	-	H-1→LUMO (45%), HOMO→L+1 (39%)	IL
	T_3	386.3	-	H-7→L+2 (12%), HOMO→L+2 (60%)	LMCT/IL/L'MCT
	S_1	357.4	0.0039	HOMO→L+1 (28%). HOMO→L+2 (61%)	IL/LMCT
	S_2	**350.2**	**0.235**	**HOMO→LUMO (87%)**	**IL**
	S_3	350.0	0.0282	H-1→L+1 (43%). H-1→L+2 (48%)	IL/LMCT
	S_4	344.9	0.0612	H-1→LUMO (90%)	IL
	S_5	338.5	0.0479	HOMO→L+1 (65%). HOMO→L+2 (26%)	IL/LMCT
	S_6	**333.7**	**0.174**	**H-1→L+1 (43%). H-1→L+2 (46%)**	**IL/LMCT**
	S_7	328.4	0.014	H-4→L+1 (17%). H-4→L+2 (14%). H-3→L+1 (19%). H-3→L+2 (15%)	IL/L'LCT/L'MCT/ LMCT
	S_8	326.2	0.012	H-4→LUMO (20%). H-3→LUMO (48%)	IL/L'LCT
	S_9	324.7	0.002	H-7→L+1 (11%). H-7→L+2 (14%). H-6→LUMO (15%). H-5→L+1 (27%). H-5→L+2 (25%)	IL/L'LCT/L'MCT
	S_{10}	322.7	0.049	H-7→LUMO (12%). H-6→L+1 (29%). H-6→L+2 (19%). H-5→LUMO (15%)	IL/L'LCT/L'MCT/ MLCT
	S_{11}	320.5	0.001	H-7→L+1 (10%). H-7→L+2 (14%). H-3→LUMO (22%). H-2→L+1 (27%)	IL/L'LCT/L'MCT
	S_{12}	319.0	0.119	H-3→L+1 (14%). H-2→LUMO (71%)	IL/L'LCT
3	T_1	469.7	-	H-1→L+1 (40%). HOMO→LUMO (49%)	IL
	T_2	469.2	-	H-1→LUMO (49%). HOMO→L+1 (41%)	IL
	T_3	378.3	-	H-3→L+1 (35%). H-2→LUMO (46%)	IL
	S_1	**351.8**	**0.2257**	**HOMO→LUMO (92%)**	**IL**
	S_2	349.6	0.0141	HOMO→L+1 (38%). HOMO→L+2 (54%)	IL/LMCT
	S_3	343.2	0.0904	H-1→LUMO (96%)	IL
	S_4	341.2	0.0897	H-1→L+1 (53%). H-1→L+2 (43%)	IL/LMCT
	S_5	335.6	0.0492	HOMO→L+1 (56%). HOMO→L+2 (37%)	IL/LMCT
	S_6	**327.7**	**0.1939**	**H-1→L+1 (43%). H-1→L+2 (51%)**	**IL/LMCT**
	S_7	320.7	0.0434	H-4→LUMO (15%). H-3→L+1 (18%). H-2→LUMO (54%)	IL/L'LCT
	S_8	320.4	0.0286	H-5→LUMO (14%). H-3→LUMO (59%). H-2→L+1 (13%)	IL/L'LCT

	S_9	314.1	0.1114	H-5→L+1 (10%). H-4→LUMO (60%). H-2→LUMO (20%)	IL/L'LCT
	S_{10}	312.6	0.0229	H-5→LUMO (47%). H-4→L+1 (24%). H-3→LUMO (16%)	IL/L'LCT
	S_{11}	310.5	0.0042	H-4→L+1 (12%). H-4→L+2 (15%). H-2→L+1 (33%). H-2→L+2 (18%)	IL/L'LCT/LMCT/ L'MCT
	S_{12}	309.5	0.0119	H-5→L+1 (12%). H-3→L+1 (46%). H-3→L+2 (11%). H-2→LUMO (18%)	IL/L'LCT/LMCT
4^{2+}	**T_1**	470.9	-	H-1→L+1 (32%). H-1→L+4 (10%). HOMO→L+1 (14%). HOMO→L+2 (29%)	IL/LL'CT/LLCT
	T_2	470.6	-	H-1→L+2 (37%). HOMO→L+1 (20%). HOMO→L+2 (15%). HOMO→L+4 (10%)	IL/LL'CT/LLCT
	T_3	432.3	-	H-1→L+1 (32%). H-1→L+4 (10%). HOMO→L+1 (14%). HOMO→L+2 (29%)	IL/LL'CT/LLCT
	S_1	365.0	0.0009	HOMO→L+1 (14%). HOMO→L+3 (67%)	IL/LL'CT/LLCT/ LMCT
	S_2	361.5	0.0058	H-1→L+1 (14%). H-1→L+3 (61%). HOMO→LUMO (11%)	IL/LL'CT/LLCT/ LMCT
	S_3	**358.0**	**0.0234**	**HOMO→LUMO (82%)**	**LL'CT**
	S_4	357.1	0.0087	H-1→LUMO (89%)	LL'CT
	S_5	**348.6**	**0.2467**	**HOMO→L+1 (25%). HOMO→L+2 (69%)**	**IL/LLCT/LL'CT**
	S_6	345.5	0.0530	H-1→L+1 (25%). H-1→L+2 (70%)	IL/LLCT/LL'CT
	S_7	343.0	0.0512	HOMO→L+1 (56%). HOMO→L+2 (20%). HOMO→L+3 (18%)	IL/LLCT/LL'CT/ LMCT
	S_8	**341.0**	**0.2018**	**H-1→L+1 (54%). H-1→L+2 (20%). H-1→L+3 (22%)**	**IL/LLCT/LL'CT/ LMCT**
	S_9	329.9	0.0078	H-2→LUMO (92%)	LL'CT
	S_{10}	329.1	0.0027	H-3→LUMO (95%)	LL'CT
	S_{11}	325.0	0.0034	HOMO→L+3 (10%). HOMO→L+4 (79%)	IL/LL'CT/LMCT
	S_{12}	323.9	0.0805	H-1→L+4 (88%)	IL/LL'CT
5^{2+}	**T_1**	471.1	-	H-1→L+2 (34%), HOMO→L+1 (45%)	IL
	T_2	470.8	-	H-1→L+1 (46%), HOMO→L+2 (34%)	IL
	T_3	410.6	-	H-8→LUMO (36%), H-7→L+5 (19%)	IL'/L'LCT
	S_1	366.5	0.0000	H-1→LUMO (20%), HOMO→L+2 (18%), HOMO→L+3 (55%)	IL/LL'CT/LMCT
	S_2	**366.0**	**0.0009**	**HOMO→LUMO (89%)**	**LL'CT**
	S_3	364.2	0.0047	H-1→LUMO (79%), HOMO→L+3 (11%)	IL/LL'CT/LMCT
	S_4	362.1	0.0168	H-1→L+2 (26%), H-1→L+3 (58%), HOMO→LUMO (10%)	IL/LL'CT/LMCT
	S_5	**349.5**	**0.2564**	**HOMO→L+1 (93%)**	**IL**

	S_6	346.5	0.0556	H-1→L+1 (96%)	IL
	S_7	342.1	0.0445	HOMO→L+2 (73%), HOMO→L+3 (21%)	IL/LL'CT/LMCT
	S_8	**340.1**	**0.2082**	**H-1→L+2 (69%), H-1→L+3 (25%)**	**IL/LL'CT**
	S_9	338.6	0.0116	H-5→LUMO (26%), H-5→L+4 (65%)	IL'
	S_{10}	335.7	0.0045	H-2→LUMO (98%)	LL'CT
	S_{11}	335.3	0.0004	H-3→LUMO (98%)	LL'CT
	S_{12}	324.5	0.0001	H-3→L+1 (10%), H-2→L+2 (33%), H-2→L+3 (20%), HOMO→L+5 (22%)	IL/LL'CT/LMCT
6^{2+}	**T_1**	530.5	-	HOMO→LUMO (59%). HOMO→L+1 (13%). HOMO→L+4 (21%)	IL'CT/L'LCT/ L'MCT
	T_2	513. 7	-	HOMO→LUMO (22%). HOMO→L+4 (56%)	IL'CT/L'LCT
	T_3	470.8	-	H-2→L+1 (33%). H-2→L+2 (28%). H-1→L+1 (12%)	IL/LLCT/LMCT
	S_1	**444.4**	**0.0377**	**HOMO→LUMO (87%). HOMO→L+1 (11%)**	**IL'CT/L'LCT**
	S_2	406.3	0.0004	HOMO→LUMO (12%). HOMO→L+1 (81%)	IL'CT/L'LCT
	S_3	405.4	0.0045	HOMO→L+2 (71%). HOMO→L+3 (22%)	IL'CT/L'LCT/ L'MCT
	S_4	392.9	0.0063	HOMO→L+2 (21%). HOMO→L+3 (77%)	IL'CT/L'LCT/ L'MCT
	S_5	363.8	0.0012	H-1→L+2 (17%). H-1→L+3 (64%)	IL/LLCT/LL'CT/ LMCT
	S_6	**363.3**	**0.0901**	**HOMO→L+4 (93%)**	**IL'CT**
	S_7	359.9	0.0082	H-2→L+2 (20%). H-2→L+3 (62%)	IL/LLCT/LL'CT/ LMCT
	S_8	352.7	0.0678	H-2→LUMO (27%). H-1→LUMO (69%)	IL/LL'CT
	S_9	351.4	0.0134	H-2→LUMO (71%). H-1→LUMO (26%)	IL/LL'CT
	S_{10}	**347.0**	**0.2016**	**H-2→L+1 (11%). H-1→L+1 (81%)**	**IL/LL'CT**
	S_{11}	344.1	0.0534	H-2→L+1 (81%). H-1→L+1 (12%)	IL/LL'CT
	S_{12}	340.0	0.0725	H-1→L+2 (67%). H-1→L+3 (19%)	IL/LLCT/LL'CT/ LMCT

Table S6. Composition (%) of Frontier MOs in terms of ligands and metals in the ground state in CH_2Cl_2.

2						
Orbital	**Energy (eV)**	**Pt**	**pbt(1)**	**pbt(2)**	**Cl(1)**	**Cl(2)**
LUMO+3	-1.44	31	27	27	7	7
LUMO+2	-2.11	41	28	28	2	2
LUMO+1	-2.35	6	46	46	1	1
LUMO	-2.41	3	47	47	1	1
HOMO	-6.54	6	48	44	1	2
HOMO-1	-6.56	1	45	49	3	3
HOMO-2	-6.85	1	42	46	6	5
HOMO-3	-6.86	1	27	23	24	25
3						
Orbital	**Energy (eV)**	**Pt**	**pbt(1)**	**pbt(2)**	**CF_3CO_2(1)**	**CF_3CO_2 (2)**
LUMO+3	-1.26	33	28	28	6	6
LUMO+2	-2.02	44	27	27	1	1
LUMO+1	-2.33	4	47	47	0	0
LUMO	-2.43	4	47	47	1	1
HOMO	-6.54	5	46	46	1	1
HOMO-1	-6.57	1	49	49	0	0
HOMO-2	-6.88	2	46	46	3	3
HOMO-3	-6.89	1	43	43	6	6
4^{2+}						
Orbital	**Energy (eV)**	**Pt**	**pbt(1)**	**pbt(2)**	**phen**	
LUMO+3	-3.05	36	21	21	22	
LUMO+2	-3.20	5	10	75	10	
LUMO+1	-3.20	5	69	5	21	
LUMO	-3.31	2	3	2	94	
HOMO	-7.31	3	45	52	0	
HOMO-1	-7.31	1	53	46	1	
HOMO-2	-7.62	1	76	19	4	
HOMO-3	-7.62	1	21	78	1	
5^{2+}						
Orbital	**Energy (eV)**	**Pt**	**pbt(1)**	**pbt(2)**	**pyraphen**	
LUMO+3	-3.07	36	22	22	20	
LUMO+2	-3.21	6	36	36	22	
LUMO+1	-3.23	5	45	45	5	
LUMO	-3.40	1	1	1	97	
HOMO	-7.33	2	49	49	0	
HOMO-1	-7.33	1	49	50	0	
HOMO-2	-7.63	1	49	49	0	
HOMO-3	-7.63	1	49	49	1	

6^{2+}					
Orbital	**Energy (eV)**	**Pt**	**pbt(1)**	**pbt(2)**	**NH_2-phen**
LUMO+5	-2.22	32	28	27	13
LUMO+4	-2.80	0	4	4	91
LUMO+3	-3.01	40	28	27	5
LUMO+2	-3.15	6	30	56	8
LUMO+1	-3.17	5	47	28	20
LUMO	-3.24	2	11	7	80
HOMO	-6.69	0	0	0	99
HOMO-1	-7.29	2	13	85	0
HOMO-2	-7.30	1	86	13	0
HOMO-3	-7.60	1	29	70	0
HOMO-4	-7.61	1	70	29	1
HOMO-5	-7.87	10	39	48	3

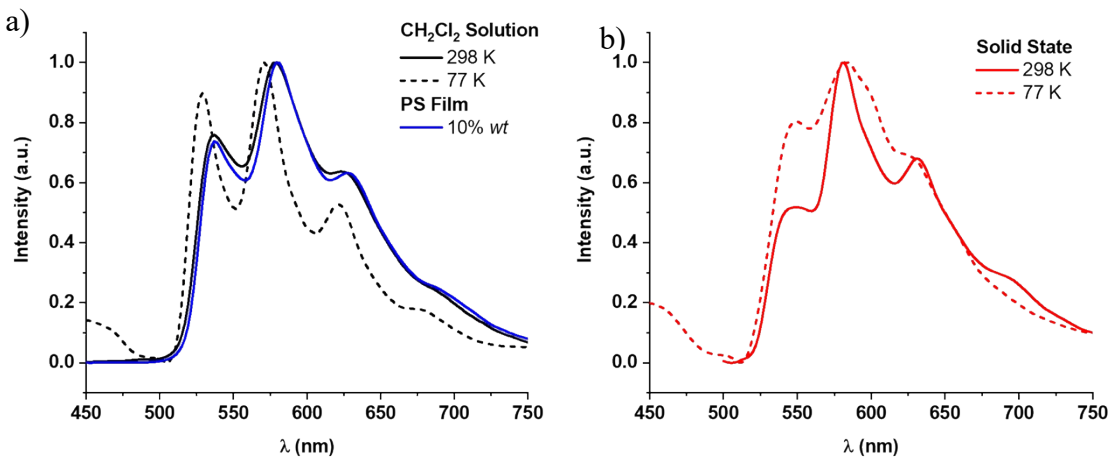

Figure S15. Emission spectra of the precursor **1** in several media.

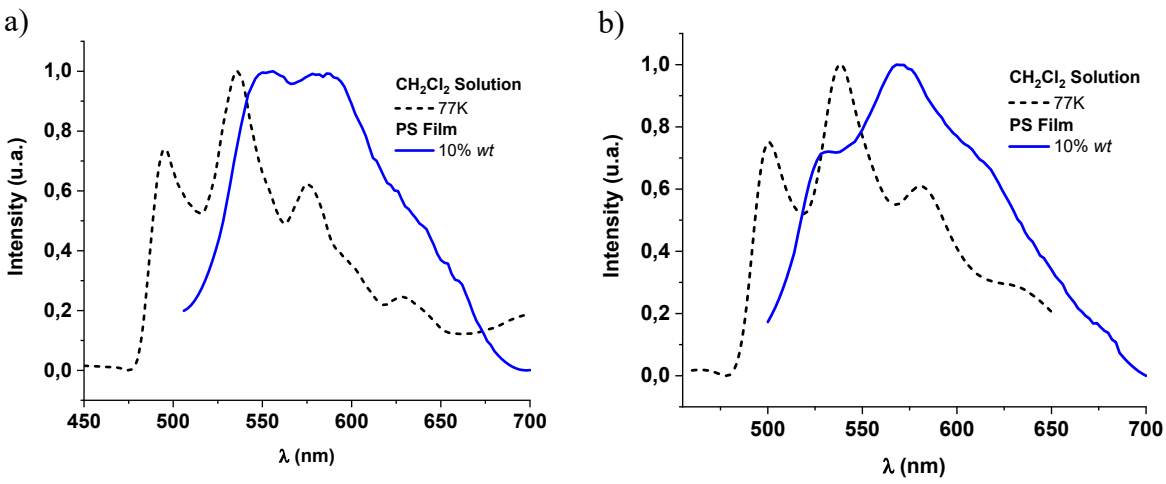

Figure S16. Emission spectra in CH_2Cl_2 glasses (77 K) and PS film 10% *wt* of a) **4-PF$_6$**, b) **5-PF$_6$**

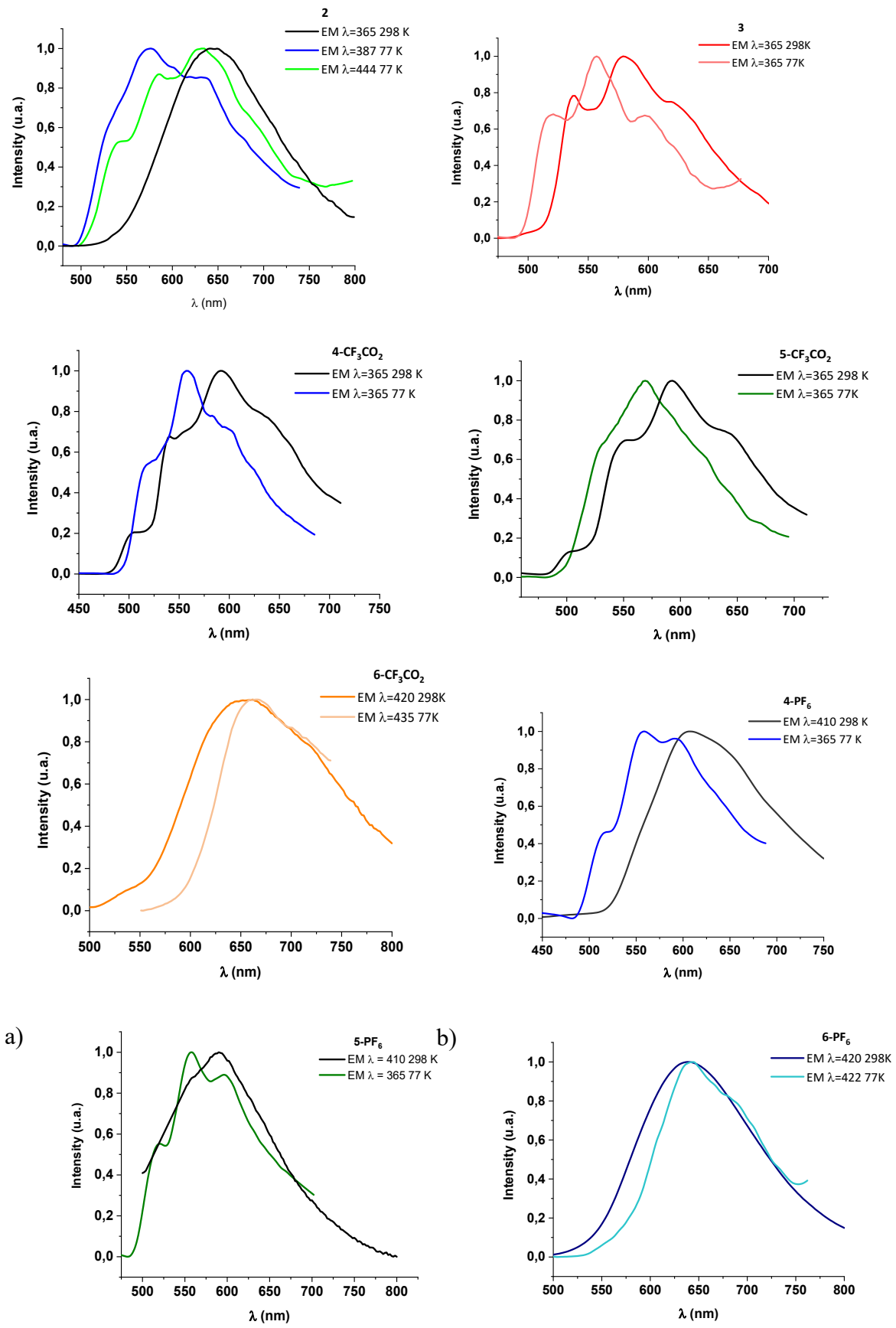

Figure S17. Emission and excitation spectra in solid state at 298 K, 77 K of a) **2**, b) **3**, c) **4-CF_3CO_2**, d) **5-CF_3CO_2**, e) **6-CF_3CO_2**, f) **4-PF_6**, g) **5-PF_6** and h) **6-PF_6**.

Table S7. Plots and composition (%) of the frontier MOs and spin density of the first triplet state in CH_2Cl_2.

2		
SOMO	SOMO-1	Spin density
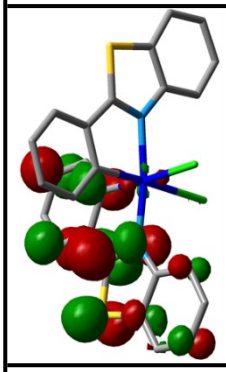	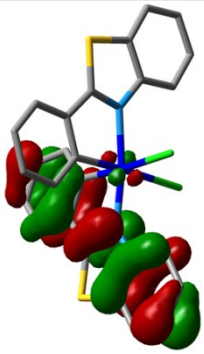	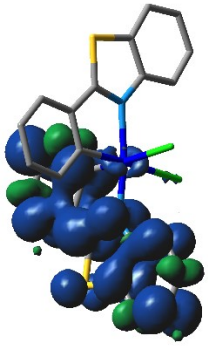
-3.97eV Pt 2 %, pbt(1) 96 %, pbt(2) 1 %, Cl(1) 0 %, Cl(2) 1 %	-5.10 eV Pt 2 %, pbt(1) 97 %, pbt(2) 0 %, Cl(1) 0 %, Cl(2) 0 %	0.014 on **Pt**
3		
SOMO	SOMO-1	Spin density
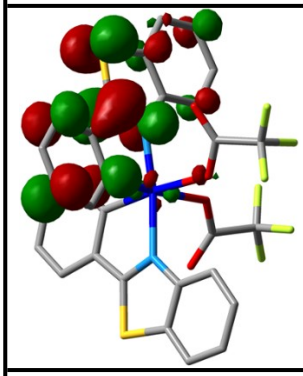	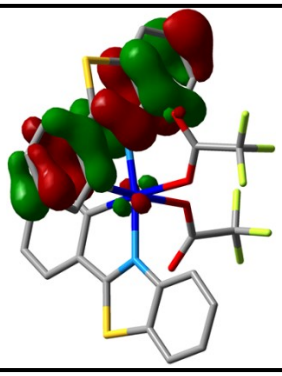	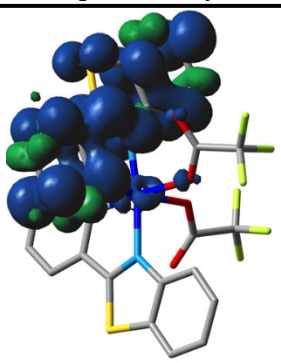
-4.17 eV Pt 2 %, pbt(1) 0 %, pbt(2) 97 %, TFA(1) 0 %, TFA(2) 1 %	-5.10 eV Pt 2 %, pbt(1) 0 %, pbt(2) 96 %, TFA(1) 0 %, TFA(2) 1 %	0.0197 on **Pt**
4^{2+}		
SOMO	SOMO-1	Spin density
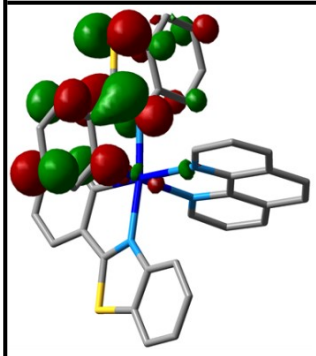	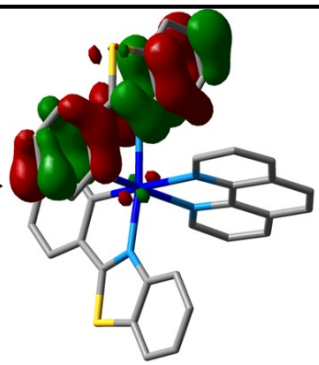	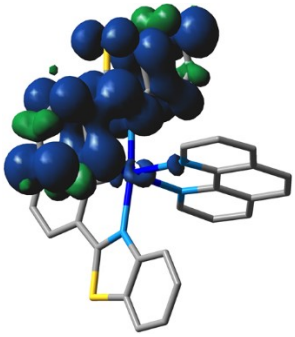
-4.92 eV Pt 2 %, pbt(1) 0 %, pbt(2) 96 %, phen 1 %	-6.21 eV Pt 1 %, pbt(1) 0 %, pbt(2) 98 %, phen 1 %	0.0128 on **Pt**

5^{2+}		
SOMO	SOMO-1	Spin density
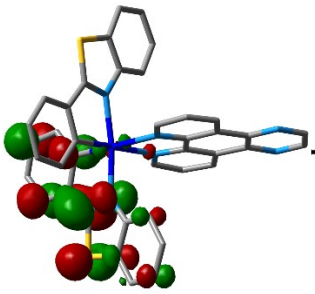	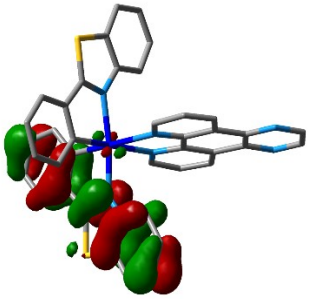	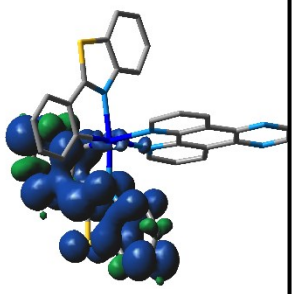
-4.94 eV Pt 2 %, pbt(1) 96 %, pbt(2) 0 %, pyraphen 1 %	-5.68 eV Pt 1 %, pbt(1) 98 %, pbt(2) 0 %, pyraphen 0 %	0.0126 on **Pt**
6^{2+}		
SOMO	SOMO-1	Spin density
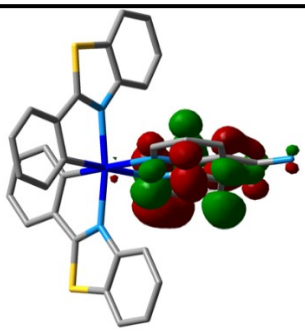	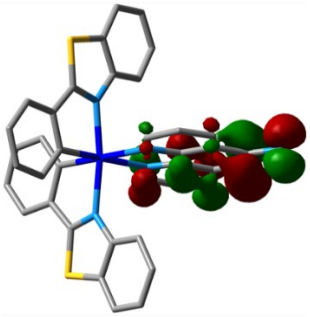	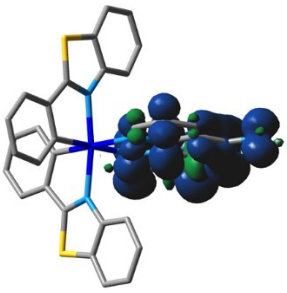
-4.57 eV Pt 1 %, pbt(1) 0 %, pbt(2) 0 %, NH_2-phen 98 %	-5.23 eV Pt 0 %, pbt(1) 0 %, pbt(2) 0 %, NH_2-phen 99 %	0.0004 on **Pt**

Table S8. Theoretical calculated energies

	2	**3**	**4^{2+}**	**5^{2+}**	**6^{2+}**
λ_{ex} ($S_0 \rightarrow T_1$)[a]	469	470	471	471	531
λ_{ex} ($S_0 \rightarrow T_2$)[a]	469	469	471	471	514
λ_{ex} ($S_0 \rightarrow T_3$)[a]	386	378	432	411	471
λ_{em} (T_1)[b]	679	685	670	670	739
λ_{em} (T_2)[b]	679	685	670	653	738
λ_{em} (T_3)[b]	[c]	439	600	516	669

[a] Vertical excitation energy by TD-DFT calculations. [b]Emission wavelength calculated by the difference between the energies of the optimized triplet states and the singlet state at the triplet geometry. [c]Overestimated value surely by the great metallic contribution on this excited state.

Table S9. Electronic energies (Hartrees) of the optimized structures in CH_2Cl_2 solution

Complex	**S_0**	**T_1**	**T_2**	**T_3**
2	-2946.017677	-2945.935085	-2945.935085	-2945.931475
3	-3077.970025	-3077.887823	-3077.887823	-3077.857419
4^{2+}	-2596.895257	-2596.812512	-2596.812512	-2596.803149
5^{2+}	-2782.615907	-2782.533229	-2782.533228	-2782.512883
6^{2+}	-2652.259441	-2652.187012	-2652.187011	-2652.176758

5. Electrochemical Properties

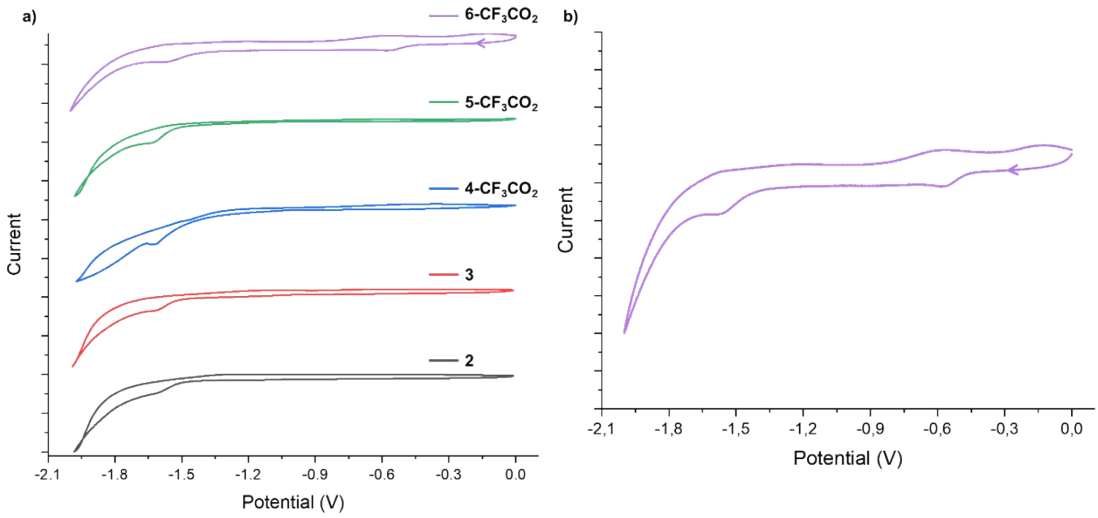

Figure S18. a) Cyclic voltammograms of the Pt^{IV} complexes in CH_2Cl_2 solution at 100 mVs^{-1}. b) expanded CV of **6-CF_3CO_2**.